

NEA/NSC/DOC(99)10  
INDC(Ger)-045  
Jül-3660

# PROGRESS REPORT ON NUCLEAR DATA RESEARCH IN THE FEDERAL REPUBLIC OF GERMANY

for the Period April 1, 1998 to March 31, 1999

June 1999

Edited by  
S. M. Qaim  
Forschungszentrum Jülich GmbH  
Institut für Nuklearchemie  
Jülich, Federal Republic of Germany

NEA/NSC/DOC(99)10  
INDC(Ger)-045

Jül-3660  
Berichte des Forschungszentrums Jülich; 3660

Edited by: S.M. Qaim  
Forschungszentrum Jülich GmbH  
Institut für Nuklearchemie  
Jülich, Federal Republic of Germany

## FOREWORD

As in previous years, this report has been prepared to promote exchange of nuclear data research information between the Federal Republic of Germany and other member states of OECD/NEA and IAEA. It covers progress reports from the research centres at Karlsruhe and Jülich, the universities of Dresden, Hannover, Köln, Mainz, München as well as from the PTB Braunschweig. The emphasis in the work reported here is on measurement, calculation, compilation and evaluation of nuclear data for applied science programmes, such as those relevant to reactor technology, transmutation concepts, accelerator shielding and development, astrophysics research, cosmogenic and meteoritic investigations, radiation therapy, production of medically important radioisotopes, etc.

The coordination of nuclear data activities at the international level is done by two committees: the NEA-Nuclear Science Committee (NEA-NSC) and the IAEA-International Nuclear Data Committee (INDC). The present Editor has the privilege and the responsibility of representing Germany in both the committees. This report should therefore also serve as a background information to some areas of work of those committees.

Each contribution is presented under the laboratory heading from where the work is reported. The names of other participating laboratories are also mentioned. When the work is relevant to the World Request List for Nuclear Data, WREND 93/94 (INDC(SEC)-104/U+G), the corresponding identification numbers are given.

Jülich, June 1999

S.M. Qaim

This document contains information of a preliminary nature. Its contents should be used with discretion.

## CONTENTS

### FORSCHUNGSZENTRUM KARLSRUHE INSTITUT FÜR KERNPHYSIK

Page

1. The (n, $\gamma$ ) Cross Section of  $^7\text{Li}$   
M. Heil, F. Käppeler, M. Wiescher, A. Mengoni 1
2. Neutron Capture of  $^{26}\text{Mg}$  at Thermonuclear Energies  
P. Mohr, H. Beer, H. Oberhummer, G. Staudt 1
3. Neutron Capture of  $^{26}\text{Mg}$  at  $kT = 52$  keV and the Resonance at  $E_n = 68.7$  keV  
P. Mohr, H. Beer, H. Oberhummer, W. Rochow, P.V. Sedyshev,  
S. Volz, A. Zilges 2
4. Neutron Capture of  $^{46}\text{Ca}$  at Thermonuclear Energies  
P. Mohr, P.V. Sedyshev, H. Beer, W. Stadler, H. Oberhummer,  
Yu. P. Popov, W. Rochow 2
5. Proton Capture Cross Sections of the Ruthenium Isotopes  
J. Bork, H. Schatz, F. Käppeler, T. Rauscher 3
6. On the Puzzling Origin of the Rare In and Sn Isotopes  
Ch. Theis, F. Käppeler, K. Wisshak, F. Voss 4
7. Neutron Capture Resonances in  $^{142}\text{Nd}$  and  $^{144}\text{Nd}$   
K. Wisshak, F. Voss, F. Käppeler 4
8. Stellar Neutron Capture Cross Sections of the Pr and Dy Isotopes  
F. Voss, K. Wisshak, F. Voss, C. Arlandini, F. Käppeler, L. Kazakov, T. Rauscher 5
9. Lifetime Measurement in  $^{176}\text{Lu}$  and its Astrophysical Consequences  
C. Doll, H.G. Börner, S. Jaag, F. Käppeler, W. Andrejtscheff 6
10. Coulomb Excitation of  $^{180}\text{Ta}$   
M. Schumann, F. Käppeler, R. Böttger, H. Schölermann 6
11. Current Quests in Nuclear Astrophysics and Experimental Approaches  
F. Käppeler, M. Wiescher, F.-K. Thielemann 7

**FORSCHUNGSZENTRUM KARLSRUHE  
INSTITUT FÜR NEUTRONENPHYSIK UND REAKTORTECHNIK**

Page

Integral Data Testing and Sensitivity/Uncertainty Analysis  
of the EFF-3 Beryllium Data Evaluations  
U. Fischer, R. Perel, Y. Wu

8

**INSTITUT FÜR NUKLEARCHEMIE  
FORSCHUNGSZENTRUM JÜLICH**

1. Isomeric Cross Sections  
S. Sudár, A. Hohn, A. Fessler, S.M. Qaim 13
2. Neutron Activation Cross Sections  
C. Nesaraja, A. Fessler, P. Reimer, S. Sudár, F. Cserpák, M. Ibn Majah,  
S.M. Qaim 14
3. Charged Particle Induced Reaction Cross Sections  
A. Hohn, S. Kastleiner, E. Heß, B. Scholten, F.M. Nortier, I.W. Schroeder,  
T.N. van der Walt, H.H. Coenen, S.M. Qaim 17

**INSTITUT FÜR KERN- UND TEILCHENPHYSIK  
TECHNISCHE UNIVERSITÄT DRESDEN**

1. Neutron and Photon Flux Spectra in an ITER Streaming Experiment  
U. Fischer, H. Freiesleben, W. Hansen, D. Richter, K. Seidel, S. Unholzer 21
2. Radioactivities induced in Fusion Reactor Structural Materials  
by 14 MeV Neutrons  
R. A. Forrest, H. Freiesleben, V.D. Kovalchuk, D.V. Markovskij, D. Richter,  
K. Seidel, V.I. Tereshkin, S. Unholzer 24

**ABTEILUNG NUKLEARCHEMIE, UNIVERSITÄT ZU KÖLN  
AND  
ZENTRUM FÜR STRAHLENSCHUTZ UND RADIOÖKOLOGIE  
UNIVERSITÄT HANNOVER**

Cross Section Measurements for the Production of  
Residual Nuclei by Medium-Energy Nucleons  
J. Protoschill, M. Gloris, S. Neumann, R. Michel, J. Kuhnhehn, U. Herpers,  
O. Jonsson, P. Malmberg, P.W. Kubik, I. Leya, E. Gilabert, B. Lavielle

26

**INSTITUT FÜR KERNCHEMIE  
UNIVERSITÄT MAINZ**

Page

Shell Effects in the Very Asymmetric Fission of  $^{242m}\text{Am}$  by Thermal Neutrons  
I. Tsekhanovitch, H.O. Denschlag, M. Davi, Z. Büyükmumcu, M. Wöstheinrich,  
F. Gönnerwein, S. Oberstedt,

35

**PHYSIK DEPARTMENT DER  
TECHNISCHEN UNIVERSITÄT MÜNCHEN  
FRM-REAKTORSTATION GARCHING**

Theoretical Evaluation of Neutron-nucleus Scattering Parameters  
from Experimental Data in the  $6 \leq A < 60$  Mass Region  
A. Aleksejevs, S. Barkanova, J. Tambergs, T. Krasta, W. Waschkowski, K. Knopf

39

**PHYSIKALISCH-TECHNISCHE BUNDESANSTALT BRAUNSCHWEIG**

1. Evaluation of a 'Best Set' of Average Cross Section Measurements  
in the  $^{235}\text{U}(n_{\text{th}},f)$  Neutron Field  
W. Mannhart
2. X-Ray and  $\gamma$ -Ray Emission Probabilities and Half-Life of  $^{153}\text{Sm}$   
U. Schötzig, E. Schönfeld, E. Günther, R. Klein, H. Schrader
3. X-Ray and  $\gamma$ -Ray Emission Probabilities of  $^{169}\text{Yb}$   
E. Schönfeld, U. Schötzig, R. Klein

40

44

44

**APPENDIX**

Addresses of Contributing Laboratories

49





# **FORSCHUNGSZENTRUM KARLSRUHE INSTITUT FÜR KERNPHYSIK**

## **1. The (n, $\gamma$ ) Cross Section of $^7\text{Li}^*$**

M. Heil, F. Käppeler, M. Wiescher<sup>1</sup>, A. Mengoni<sup>2</sup>

The  $^7\text{Li}(n,\gamma)^8\text{Li}$  reaction is of relevance for primordial nucleosynthesis in inhomogeneous bigbang models as well as in connection with the solar neutrino problem where the mirror reaction  $^7\text{Be}(p,\gamma)^8\text{Be}$  is responsible for the production of high energy solar neutrinos. The cross section was measured at neutron energies of  $E_n = 5$  meV and  $E_n = 54$  keV. With the present results and the reanalysis of a previous measurement the discrepancy among existing data could be resolved and the cross section be determined with improved accuracy.

\* *Ap. J.* **507** (1998) 997.

## **2. Neutron Capture of $^{26}\text{Mg}$ at Thermonuclear Energies\***

P. Mohr<sup>3</sup>, H. Beer, H. Oberhummer<sup>4</sup>, G. Staudt<sup>5</sup>

The neutron capture cross section of  $^{26}\text{Mg}$  was measured relative to the known gold cross section at thermonuclear energies using the fast cyclic activation technique. The experiment was performed at the 3.75 MeV Van de Graaff accelerator, Forschungszentrum Karlsruhe. The experimental capture cross section is the sum of resonant and direct contributions. For the resonance at  $E_{n,\text{lab}} = 220$  keV our new results are in disagreement with the data from Weigmann, Macklin, and Harvey [*Phys. Rev. C* **14**, 1328 (1976)]. An improved Maxwellian averaged capture cross section is derived from the new experimental data taking into account *s*- and *p*-wave capture and resonant contributions. The properties of so-called potential resonances which influence the *p*-wave neutron capture  $^{26}\text{Mg}$  are discussed in detail.

\* *Phys. Rev. C* **58** (1998) 932.

<sup>1</sup> University of Notre Dame, Notre Dame, IN 46556, USA

<sup>2</sup> ENEA, I-40128 Bologna, Italy

<sup>3</sup> Technical University Darmstadt, D-64289 Darmstadt, Germany

<sup>4</sup> Technical University Vienna, A-1040 Vienna, Austria

<sup>5</sup> University of Tübingen, D-72076 Tübingen, Germany

### 3. Neutron Capture of $^{26}\text{Mg}$ at $kT = 52$ keV and the Resonance at $E_n = 68.7$ keV\*

P. Mohr<sup>1</sup>, H. Beer, H. Oberhummer<sup>3</sup>, W. Rochow<sup>4</sup>, P.V. Sedyshev<sup>2</sup>, S. Volz<sup>1</sup>,  
A. Zilges<sup>1</sup>

The neutron capture cross section of  $^{26}\text{Mg}$  was measured relative to the known gold cross section at  $kT = 52$  keV using the fast cyclic activation technique. The experiment was performed at the Van de Graaff accelerator, Universität Tübingen. From the new experimental result we deduce the resonance strength for the resonance at  $E_n = 68.7$  keV which is in good agreement with a direct measurement by Weigmann et al. Finally, we calculate the Maxwellian averaged capture cross section  $\langle \sigma \rangle$  in the astrophysically relevant energy region from the available experimental data, and we discuss the discrepancies of  $\langle \sigma \rangle$  between our work and a previous calculation by Weigmann et al.

\* Phys. Rev. C, in press.

### 4. Neutron Capture of $^{46}\text{Ca}$ at Thermonuclear Energies\*

P. Mohr<sup>1</sup>, P.V. Sedyshev<sup>2</sup>, H. Beer, W. Stadler<sup>3</sup>, H. Oberhummer<sup>3</sup>, Yu. P. Popov<sup>2</sup>,  
W. Rochow<sup>4</sup>

A study of the reaction  $^{46}\text{Ca}(n,\gamma)^{47}\text{Ca}$  is of astrophysical interest, because  $^{46}\text{Ca}$  is bypassed by charged-particle reactions. The nucleus  $^{46}\text{Ca}$  is produced and destroyed by neutron-induced nucleosynthesis in hydrostatic helium, carbon and neon burning through the reaction chain  $^{45}\text{Ca}(n,\gamma)^{46}\text{Ca}(n,\gamma)^{47}\text{Ca}$ . At the Karlsruhe and Tübingen 3.75MV Van de Graaff accelerators the thermonuclear  $^{46}\text{Ca}(n,\gamma)^{47}\text{Ca}$  (4.54 d) cross section was measured by the activation technique via the 1297.09 keV  $\gamma$ -ray line of the  $^{47}\text{Ca}$  decay. Samples of  $\text{CaCO}_3$  enriched in  $^{46}\text{Ca}$  to 5 % were irradiated between two gold foils which served as capture standards using neutrons from the  $^7\text{Li}(p,n)$  and

---

<sup>1</sup> Technical University Darmstadt, D-64289 Darmstadt, Germany

<sup>2</sup> Frank Laboratory of Neutron Physics, JINR, 141980 Dubna, Moscow Region, Russia

<sup>3</sup> Technical University Vienna, A-1040 Vienna, Austria

<sup>4</sup> University of Tübingen, D-72076 Tübingen, Germany

T(p,n) reactions. The capture cross section was measured at the mean neutron energies 30, 104, 149, 180, and 215 keV, respectively. Maxwellian averaged capture cross sections were measured at the quasi-thermal neutron energies  $kT = 25$  keV and 52 keV, respectively. It was found that the  $^{46}\text{Ca}(n,\gamma)^{47}\text{Ca}$  cross section in the thermonuclear energy region and at thermal energy is dominated by an s-wave resonance at 28.4 keV with a neutron width  $\Gamma_n = (17.4^{+3.6}_{-2.8})$  keV and a radiation width  $\Gamma_\gamma = (2.4 \pm 0.3)$  eV. The stellar reaction rate is determined in the temperature range from  $kT = 1$  to 250 keV and is compared with previous investigations using Hauser-Feshbach calculations or experimental cross section data. The astrophysical consequences of the new stellar reaction rate with respect to the nucleosynthetic abundance of  $^{46}\text{Ca}$  are discussed.

\* Phys. Rev. C, in press.

## 5. Proton Capture Cross Sections of the Ruthenium Isotopes\*

J. Bork, H. Schatz<sup>5</sup>, F. Käppeler, T. Rauscher<sup>6</sup>

The proton capture cross sections of the stable ruthenium isotopes 96, 98, 99, and 104 have been measured by means of the activation method in the proton energy range between 1.5 and 3 MeV. Thin layers of natural ruthenium were irradiated at the Karlsruhe 3.75 MV Van de Graaff accelerator with proton beams of 20 to 50  $\mu\text{A}$ . The activity induced by (p, $\gamma$ ) reactions was measured with a calibrated HPGe detector. In this way, 6 (p, $\gamma$ ) cross sections for populating ground states and isomers in 4 different Rh isotopes could be determined simultaneously with systematic uncertainties of typically 4 to 5%. The fact that experimental data are almost completely missing in the  $A > 70$  region illustrates the need of checking and complementing the statistical model calculations which are so far the only data used in  $p$  process studies.

\* Phys. Rev. C 58 (1998) 524.

---

<sup>5</sup> University of Notre Dame, Notre Dame, USA; now at GSI Darmstadt, D-64291 Darmstadt, Germany

<sup>6</sup> University of Basel, CH-4056 Basel, Switzerland

## 6. On the Puzzling Origin of the Rare In and Sn Isotopes\*

Ch. Theis, F. Käppeler, K. Wisshak, F. Voss

The neutron capture cross sections of the stable isotopes  $^{106}\text{Cd}$ ,  $^{108}\text{Cd}$ ,  $^{114}\text{Cd}$ ,  $^{116}\text{Cd}$  have been measured relative to gold by means of the activation method using the quasistellar neutron spectrum for  $kT = 25$  keV that can be produced via the  $^7\text{Li}(p,n)^7\text{Be}$  reaction near threshold. These data are given with uncertainties between 3 and 6%, five times smaller than those quoted for most of the few previous experiments. The present results complement recent measurements on isotopes of tin and a discussion of the stellar  $\beta$ -decay rates in the  $A = 113/115$  region, and allow an update of the nucleosynthetic origin of the Cd/In/Sn isotopes which is complicated by the  $s$ -process branchings at  $^{113}\text{Cd}$ ,  $^{115}\text{Cd}$  and  $^{115}\text{In}$  as well as by the many isomers in this mass region. The  $s$ -process yields obtained with the classical  $s$ -process and with an AGB model exhibit a significant difference with respect to the cadmium and tin abundances with interesting consequences for the  $r$ -process residuals in this mass region. Nevertheless, the origin of the rare, odd isotopes  $^{113}\text{In}$  and  $^{115}\text{Sn}$  remains unclear. The cross sections for the two light Cd isotopes, 106 and 108, are of interest for testing Hauser-Feshbach extrapolations to the  $p$ -process region.

\* *Ap. J.* **500** (1998) 1039.

## 7. Neutron Capture Resonances in $^{142}\text{Nd}$ and $^{144}\text{Nd}$ \*

K. Wisshak, F. Voss, F. Käppeler

The neutron capture cross sections of  $^{142}\text{Nd}$  and  $^{144}\text{Nd}$  which were determined recently with the Karlsruhe  $4\pi\text{BaF}_2$  detector have been reanalyzed at low energies. The parameters of 52 resonances in  $^{142}\text{Nd}$  and of 78 resonances in  $^{144}\text{Nd}$  were extracted by means of a shape analysis program, yielding a more reliable determination of the averaged cross sections below 20 keV. This study confirms the previously reported stellar cross sections, so that the  $s$ -process study based on these data remains unchanged.

\* *Phys. Rev. C* **57** (1998) 3452.

## 8. Stellar Neutron Capture Cross Sections of the Pr and Dy Isotopes\*

F. Voss, K. Wisshak, F. Voss, C. Arlandini, F. Käppeler, L. Kazakov<sup>1</sup>,  
T. Rauscher<sup>2</sup>

The neutron capture cross sections of  $^{141}\text{Pr}$ ,  $^{160}\text{Dy}$ ,  $^{161}\text{Dy}$ ,  $^{162}\text{Dy}$ ,  $^{163}\text{Dy}$  and  $^{164}\text{Dy}$  have been measured in the energy range from 3 to 225 keV at the Karlsruhe 3.75 MV Van de Graaff accelerator. Neutrons were produced via the  $^7\text{Li}(p,n)^7\text{Be}$  reaction by bombarding metallic Li targets with a pulsed proton beam. Capture events were registered with the Karlsruhe  $4\pi$  Barium Fluoride Detector. The cross sections were determined relative to the gold standard. For the first time the correction for undetected capture events was completely obtained from experimental information, using capture cascades derived from measurements with an ADC system. The cross section ratios could be determined with an overall uncertainty of 1 – 1.5%, an average improvement compared to previous measurements by a factor of 4.

Maxwellian averaged neutron capture cross sections were calculated for thermal energies between  $kT = 8$  keV and 100 keV. For most of the isotopes there is reasonable agreement with recent evaluations, but discrepancies of  $\sim 20\%$  were observed for  $^{160}\text{Dy}$  and  $^{164}\text{Dy}$ . The experimental data were complemented by statistical model calculations in order to describe the cross section enhancements in the stellar environment.

The astrophysical implications of the present data include the quest for the origin of  $^{160}\text{Dy}$ , the decomposition of the Dy abundances in the respective  $s$ - and  $r$ -process contributions, branchings of the  $s$ -process chain at the terrestrially stable isotopes  $^{157}\text{Gd}$  and  $^{163}\text{Dy}$ , and the isotopically anomalous dysprosium in meteoritic inclusions.

\* *Phys. Rev. C* **59** (1999) 1154.

---

<sup>1</sup> Institute of Physics and Power Engineering, 242090 Obninsk, Kaluga Region, Russia

<sup>2</sup> University of Basel, CH-4056 Basel, Switzerland

## 9. Lifetime Measurement in $^{176}\text{Lu}$ and its Astrophysical Consequences\*

C. Doll<sup>1,2</sup>, H.G. Börner<sup>2</sup>, S. Jaag<sup>3</sup>, F. Käppeler, W. Andrejtscheff<sup>4</sup>

Because of its temperature-dependent half-life,  $^{176}\text{Lu}$  represents an important thermometer for the slow neutron capture process (*s* process) which accounts for the origin of about half of the abundances between Fe and Bi. This interpretation of the observed  $^{176}\text{Lu}$  abundance has been improved by a new lifetime measurement of the  $J^\pi = 5^-$  state at 838 keV in  $^{176}\text{Lu}$ . The present limit of  $\tau_{838} \geq 10$  ps provides a more stringent constraint for the thermal equilibration between the long-lived ground state ( $t_{1/2} = 41$  Gyr) and the short-lived K-isomer at 123 keV ( $t_{1/2} = 3.7$  h), and, hence, for the resulting estimate of the temperature during shell helium burning in red giant stars.

\* *Phys. Rev. C* **59** (1999) 492.

## 10. Coulomb Excitation of $^{180}\text{Ta}$ \*

M. Schumann, F. Käppeler, R. Böttger<sup>5</sup>, H. Schölermann<sup>5</sup>

The existence of a low energetic intermediate state in  $^{180}\text{Ta}$  which provides a coupling of the stable isomer and the radioactive ground state was investigated by means of Coulomb excitation. Natural tantalum foils were irradiated by protons with incident energies between 3.0 and 3.7 MeV, and with  $\alpha$ -particles in the energy range 12 - 20 MeV. Subsequently, the foils were counted for the induced ground state activity of  $^{180}\text{Ta}$ . From the thick target yields an IS between 0.6 and 2.2 MeV excitation energy was inferred. The population of the IS in the stellar environment of the *s* process depends critically on the prevailing temperatures. Current stellar models suggest *s*-process temperatures below  $3.1 \cdot 10^8$  K which lead to a negligible population of intermediate states above 1.2 MeV. Thus, the present data do not allow stringent conclusions

<sup>1</sup> Technical University Munich, D-85748 Garching, Germany

<sup>2</sup> Institut Laue-Langevin, F-38042 Grenoble Cedex 9, France

<sup>3</sup> Forschungszentrum Karlsruhe, Institute for Neutron and Reactor Physics,  
D-76021 Karlsruhe, Germany

<sup>4</sup> Bulgarian Academy of Sciences, Institute for Nuclear Research and Nuclear Energy,  
1784 Sofia, Bulgaria

<sup>5</sup> PTB Braunschweig, D-38116 Braunschweig, Germany

about the destruction of  $^{180}\text{Ta}$  under these conditions, but an  $s$  process origin seems still possible. Furthermore, the experiments support the existence of a new isomer in  $^{184}\text{Re}$ .

*Phys. Rev. C* **58** (1998) 1790.

## 11. Current Quests in Nuclear Astrophysics and Experimental Approaches\*

F. Käppeler, M. Wiescher<sup>1</sup>, F.-K. Thielemann<sup>2</sup>

This review summarizes to date's problems and questions in experimental Nuclear Astrophysics. It focuses on the present needs for experimental data emphasising novel methods and approaches. Starting with an introductory overview on nuclear energy generation and nucleosynthesis in an astrophysical plasma, the discussion concentrates on crucial problems related to the various aspects of stellar evolution, from the hydrostatic stage over the advanced burning scenarios up to and including the supernova explosion mechanism. Innovative experimental approaches are needed to pursue the associated questions in stellar nucleosynthesis. Particular emphasis is given to the potential use of radioactive ion beams and their importance for characterizing explosive nucleosynthesis in X-ray bursts and supernovae.

*Annu. Rev. Nucl. Part. Sci.* **48** (1998) 175.

---

<sup>1</sup> University of Notre Dame, Notre Dame, IN 46556, USA

<sup>2</sup> University of Basel, CH-4056 Basel, Switzerland

**FORSCHUNGSZENTRUM KARLSRUHE  
INSTITUT FÜR NEUTRONENPHYSIK U. REAKTORTECHNIK**

**Integral Data Testing and Sensitivity/Uncertainty Analysis of the EFF-3 Beryllium Data Evaluation**

U. Fischer, R. Perel<sup>1</sup>, Y. Wu<sup>2</sup>

In the framework of the European Fusion File (EFF) Project, integral data tests and sensitivity/ uncertainty analyses are being performed as part of the QA (quality assurance) procedure for new and updated EFF data evaluations. According to the EFF priorities, the main focus over the reporting period was on the new EFF-3.0 <sup>9</sup>Be evaluation by IRK Vienna.

The applied data testing methodology includes three-dimensional Monte Carlo calculations with the MCNP code to calculate the neutron leakage spectra as measured in the integral experiments considered. Graphical comparisons are being performed for neutron flux spectra and numerical comparisons are done for neutron flux integrals to provide C/E data tables. Sensitivity and uncertainty analyses include three-dimensional Monte Carlo calculations with a local update to MCNP4A for calculating sensitivities of point detector tallies [1]. With the resulting sensitivity profiles and the covariance matrices generated with the NJOY processing code from the EFF data files, uncertainties of the calculated point detector responses (neutron fluxes) due to uncertainties of the cross-section data (excitation functions) are being calculated.

For testing and qualifying the Beryllium data, the Karlsruhe Neutron Transmission Experiment (KANT) on a 17 cm thick Be spherical shell [2,3] and the FNS/JAERI time-of-flight (TOF) experiment on a 15.24 cm thick Be cylindrical slab [4] have been considered. Sensitivity/uncertainty calculations using the Monte Carlo technique for point detectors have been performed for the KANT spherical shell experiment. The neutron (leakage) multiplication factor is well reproduced with all the considered <sup>9</sup>Be data evaluations (Table 1) due to the fact that, at this thickness, it is rather insensitive

---

<sup>1</sup> Permanent address: Racah Institute of Physics, Hebrew University of Jerusalem, 91904 Jerusalem, Israel

<sup>2</sup> Permanent address: Institute of Plasma Physics, Academia Sinica, P.O. Box 1126, Hefei, P.R. China



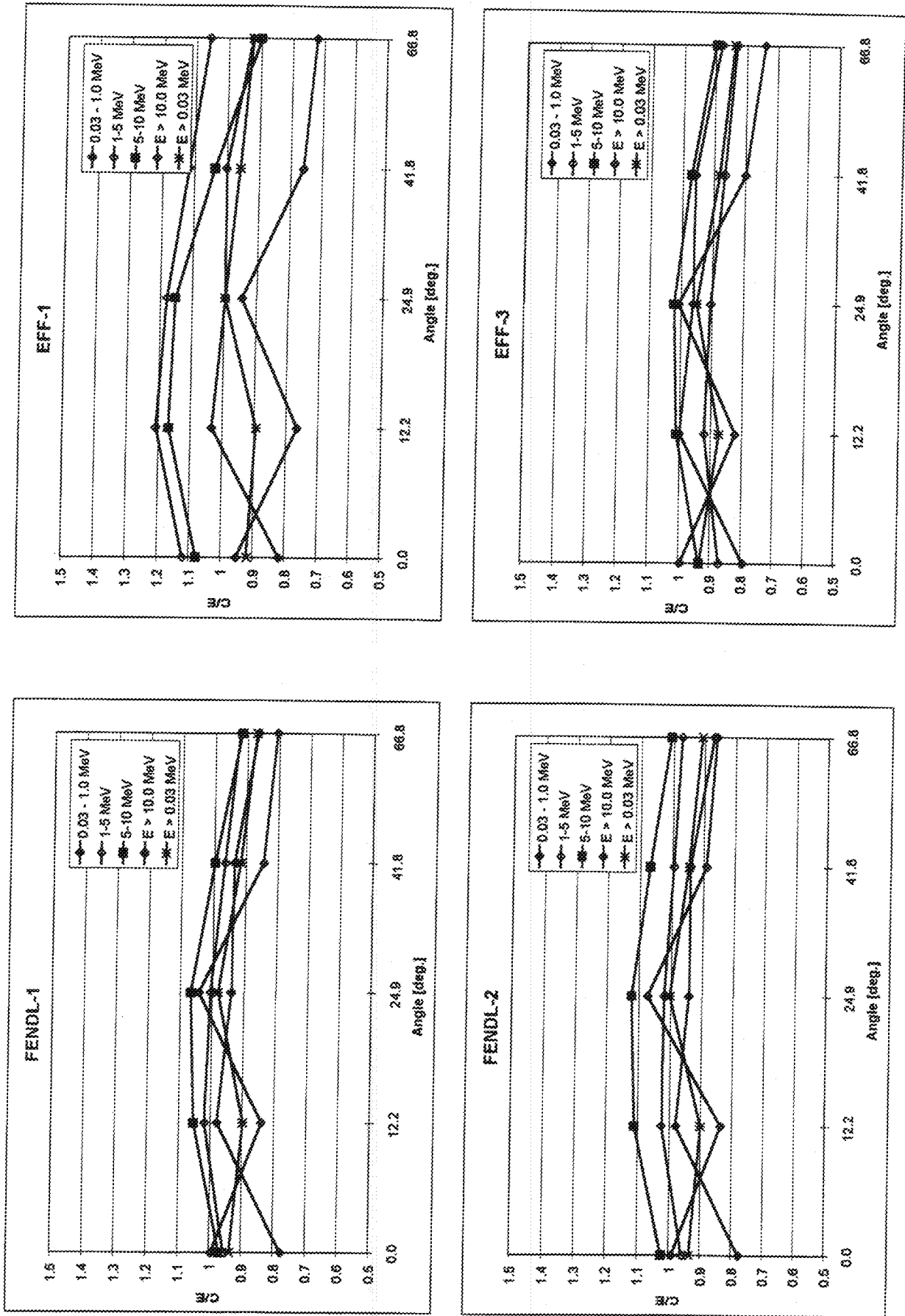


Fig. 2: FNS Beryllium slab [ $t=15.2$  cm] transmission experiment: C/E (calculation/experiment) comparison for neutron flux integrals

## References

- [1] R.L. Perel, J.J. Wagschal, and Y. Yeivin, "Monte Carlo calculation of point-detector sensitivities to material parameters", Nucl. Sci. Eng., 124 (1996) 197 - 209
- [2] U. von Möllendorff, U. Fischer, H. Fries, H. Giese, F. Kappler, R. Tayama, T. Tsukiyama and E. Wiegner, "Measurement and analysis of neutron leakage spectra from beryllium spherical shells", in: Fusion Technology 1992, Vol.2, eds. C. Ferro, M. Gaspararotto and H. Knoepfel (Elsevier 1993) pp. 1537 - 1541
- [3] U. von Möllendorff, A.V. Alevra, H. Giese, F. Kappler, H. Klein and R. Tayama, "Measurements of 14 MeV neutron multiplication in spherical beryllium shells", Fus.Eng.Des. 28 (1995) 737 - 744
- [4] Y. Oyama and H. Maekawa, Measurement and analysis of an angular neutron flux on a beryllium slab irradiated with deuterium-tritium neutrons, Nuclear Science and Engineering 97 (1987) 220 - 234

# INSTITUT FÜR NUKLEARCHEMIE FORSCHUNGSZENTRUM JÜLICH

## 1. Isomeric Cross Sections

S. Sudar\*, A. Hohn, A. Fessler†, S.M. Qaim

Some of the on-going experimental and theoretical studies on this topic were completed [cf. 1]. Measurements on the high spin states  $^{53m}\text{Fe}$  ( $I = 19/2^-$ ),  $^{195m}\text{Hg}$  ( $I = 13/2^+$ ) and  $^{197m}\text{Hg}$  ( $I = 13/2^+$ ) in neutron,  $^3\text{He}$ - and  $\alpha$ -particle induced reactions, mentioned in the last Progress Report, were also completed. Nuclear model calculations are in progress, partly in collaboration with the IRK Vienna (B. Strohmaier).

Of special interest during the last year was a study of the isomeric pair  $^{120m,g}\text{I}$ . The ground state ( $I = 2^-$ ) is potentially interesting for Positron Emission Tomography. In order to estimate the level of the interfering  $^{120m}\text{I}$ , we determined the excitation functions for the formation of the two states as well as their isomeric cross section ratios ( $\frac{\sigma_m}{\sigma_m + \sigma_g}$ ) in three reactions, namely,  $^{122}\text{Te}(p,3n)^{120m,g}\text{I}$ ,  $^{120}\text{Te}(p,n)^{120m,g}\text{I}$  and  $^{120}\text{Te}(d,2n)^{120m,g}\text{I}$ . The ratio was found to be the highest in the (p,3n) reaction and the lowest in the (p,n) reaction. In order to interpret the experimental data, nuclear model calculations were performed using the code STAPRE. Whereas the ground state cross section could be reproduced rather well by the calculation, there was considerable difficulty in describing the metastable state. The major reason for the latter was the uncertainty in the spin and parity. A series of calculations with spins between 4 and 8, and for both even and odd parity, was performed. The results showed strong variations. Assuming a spin of  $4^+$  for the metastable state, the isomeric cross section ratio could be described in all the above mentioned reactions. Experimental and theoretical studies on isomeric cross section ratios thus help in the characterization of nuclear level structure.

---

\* Institute of Experimental Physics, Kossuth University, Debrecen, Hungary

† IRMM, Geel, Belgium

## 2. Neutron Activation Cross Sections

C. Nesaraja, A. Fessler<sup>†</sup>, P. Reimer<sup>†</sup>, S. Sudár\*, F. Cserpák\*, M. Ibn Majah<sup>††</sup>,  
S.M. Qaim

(Relevant to request identification numbers: 86 11 82 F, 92 10 04 F, 92 10 09 M,  
92 10 56 R, 92 10 57 R, 92 10 68 R)

In continuation of our radiochemical studies on neutron induced reactions, especially over the energy range of 5 to 12 MeV [cf. 2], we completed cross section measurements on several isotopes of Cr, Ni, Zn, Ga and Ge. The reactions  $^{58}\text{Ni}(n,\alpha)^{55}\text{Fe}$  and  $^{50}\text{Cr}(n,n'p)^{49}\text{V}$  were investigated in co-operation with the IRMM Geel. They had a common feature: the products decay by pure EC and thus had to be characterized by soft x-ray spectrometry. Of particular interest were the results for the  $^{58}\text{Ni}(n,\alpha)^{55}\text{Fe}$  reaction since there existed a longstanding discrepancy between the activation and  $\alpha$ -detection data. A summary of the results is given in Fig. 1. In the left hand diagram the discrepancy is evident. In the right hand diagram the older activation results were renormalized, the present data were added, and the region between 4 and 13 MeV was expanded. The discrepancy appears to be resolved since now most of the data agree within the limits of errors. The results of nuclear model calculations are also in agreement with the experimental data (for a detailed study on these reactions cf. [3]).

Investigations on Zn, Ga and Ge involved experimental and theoretical studies of excitation functions of  $^{70}\text{Ge}(n,p)^{70}\text{Ga}$ ,  $^{73}\text{Ge}(n,p)^{73}\text{Ga}$ ,  $^{74}\text{Ge}(n,p)^{74}\text{Ga}$ ,  $^{71}\text{Ga}(n,p)^{71m}\text{Zn}$ ,  $^{71}\text{Ga}(n,2n)^{70}\text{Ga}$ ,  $^{67}\text{Zn}(n,p)^{67}\text{Cu}$  and  $^{68}\text{Zn}(n,\alpha)^{65}\text{Ni}$  reactions. For most of the reactions, our measurements provide the first consistent sets of data near their thresholds. In most of the cases, the results of nuclear model calculations agreed fairly well with the experimental data. The results for several isotopes of Ge (obtained in this work and reported in the literature) led to an analysis of some systematic trends in (n,p) excitation functions. The results are reproduced in Fig. 2. Obviously, with the increasing

<sup>†</sup> Mainly at IRMM, Geel, Belgium

<sup>††</sup> CNESTEN, Rabat, Morocco

\* Institute of Experimental Physics, Kossuth University, Debrecen, Hungary

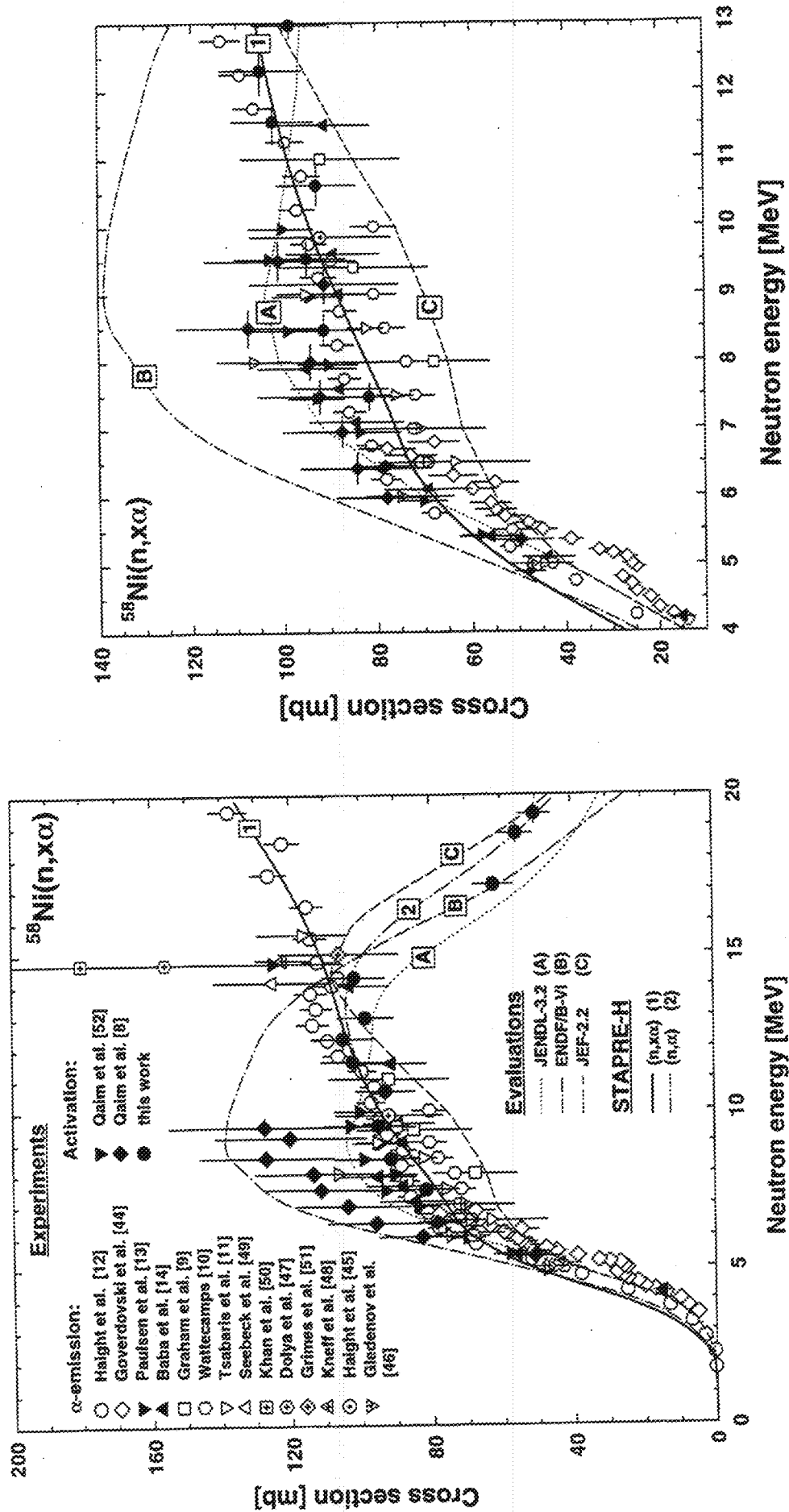


Fig. 1 Excitation functions of the  $^{58}\text{Ni}(n,\alpha)^{55}\text{Fe}$  and  $^{58}\text{Ni}(n,\alpha)$  reactions. The data for the  $(n,\alpha)$  reaction were obtained by the activation technique and those for the  $(n,\alpha)$  process via detection of emitted  $\alpha$ -particles. Left hand side: all data as reported; right hand side: expanded scale with emitted charged particle data, present activation data and renormalized old activation data (for more details cf. [3]).

target mass number, the threshold of the (n,p) reaction increases and the cross section at a given neutron energy decreases. It can be understood in terms of the increasing tendency of neutron emission as the target nucleus becomes more neutron excess. As far as the results of model calculations are concerned, the preequilibrium component increases with the increasing neutron energy (for a more detailed description of these reactions cf. [4]).

Among other measurements, data on the reactions  $^{107}\text{Ag}(n,\alpha)^{104\text{m,g}}\text{Rh}$  and  $^{109}\text{Ag}(n,\alpha)^{106\text{m,g}}\text{Rh}$  are being refined and radiochemical work on  $^{91}\text{Zr}(n,p)^{91}\text{Y}$  and  $^{92}\text{Zr}(n,\alpha)^{89}\text{Sr}$  reactions is continuing. Furthermore, a project on the formation of long-lived activities, e.g. via  $^{94}\text{Mo}(n,p)^{94}\text{Nb}$  ( $T_{1/2} = 2 \times 10^4 \text{ a}$ ) and  $^{204}\text{Pb}(n,p)^{204}\text{Tl}$  ( $T_{1/2} = 3.78 \text{ a}$ ) reactions, has been initiated in collaboration with the IRMM Geel (A. Plompen). Very clean radiochemical separations and low-level  $\beta^-$  or  $\gamma$ -counting will be mandatory.

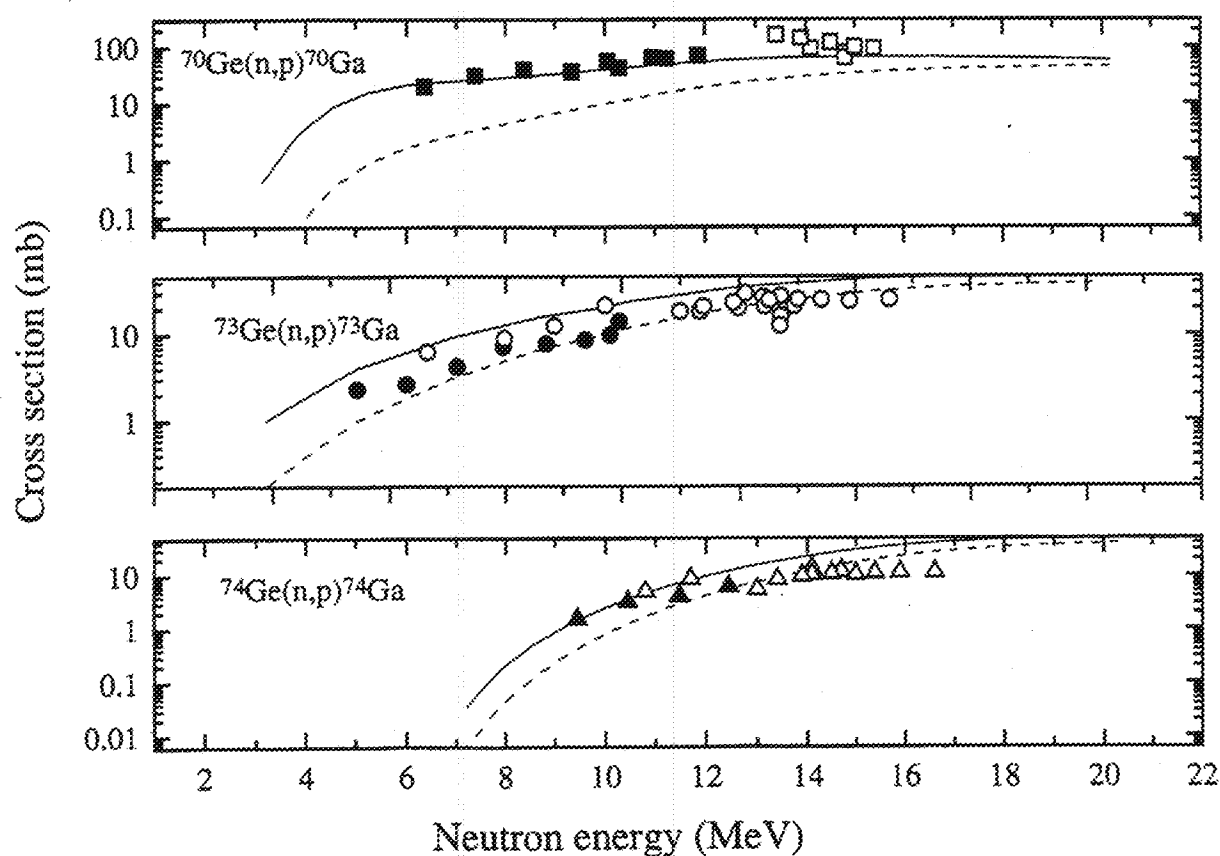


Fig. 2 Systematic trends in experimental and calculated excitation curves for (n,p) reactions on  $^{70,73,74}\text{Ge}$ . Broken lines indicate preequilibrium contributions and solid lines the sum of preequilibrium and equilibrium components.

### 3. Charged Particle Induced Reaction Cross Sections

A. Hohn, S. Kastleiner, E. Heß, B. Scholten, F.M. Nortier\*, I.W. Schroeder\*, T.N. van der Walt\*, H.H. Coenen, S.M. Qaim

In continuation of our systematic studies on charged particle induced reaction cross section data for medical applications [cf. 5 - 8], during the present report following activities were pursued:

*a) Measurement of excitation functions relevant to the production of the positron emitters  $^{18}\text{F}$ ,  $^{83}\text{Sr}$ ,  $^{120\text{g}}\text{I}$  and  $^{124}\text{I}$*

In connection with the  $^{18}\text{F}$  ( $T_{1/2} = 110$  min) production via the  $^{18}\text{O}(\text{p},\text{n})^{18}\text{F}$  reaction (see last Progress Report) we performed some more measurements in the proton energy range of 8 to 14 MeV. Further measurements are planned near the threshold of the reaction (3 - 4 MeV) in collaboration with the ATOMKI, Debrecen, Hungary.

The radioisotope  $^{83}\text{Sr}$  ( $T_{1/2} = 32.4$  h) is a positron emitting analogue of the commonly used therapy radioisotope  $^{89}\text{Sr}$ .  $^{83}\text{Sr}$  appears to be especially suited for dosimetry and therapy planning via PET. It is produced in small amounts via the  $^{82}\text{Kr}(\text{}^3\text{He}, 2\text{n})^{83}\text{Sr}$  reaction. For optimising the production via the  $^{85}\text{Rb}(\text{p}, 3\text{n})^{83}\text{Sr}$  reaction, work was initiated on the determination of the excitation function up to 70 MeV. Thin samples of highly enriched  $^{85}\text{RbCl}$  were prepared via a sedimentation technique and irradiations were done at the two cyclotrons in Jülich (CV 28 and Injector of COSY) as well as at the Accelerator in PSI (Villigen, Switzerland). Detailed data analysis is in progress. First results show that  $^{83}\text{Sr}$  can be produced in sufficient quantities at a medium-sized cyclotron.

As described in the last Progress Report, the radioisotope  $^{120\text{g}}\text{I}$  ( $T_{1/2} = 81$  min) can

---

\* National Accelerator Centre (NAC), Faure, South Africa

be produced via the middle-energy  $^{122}\text{Te}(p,3n)$ -reaction as well as via the low-energy  $^{120}\text{Te}(p,n)$ -reaction. Now we investigated the  $^{120}\text{Te}(d,2n)$ -process. From the viewpoint of production yield and isotopic purity this reaction is unsuitable. However, considering the isomeric purity, this process lies between the above mentioned two reactions. A comparison of the three routes is given in Table 1. Evidently, the  $^{120}\text{Te}(p,n)$ -process is most suitable for the production of  $^{120g}\text{I}$ : the purity of the product is highest and a small cyclotron ( $E_p \leq 20$  MeV) is adequate.

The longer-lived  $\beta^+$  emitting radioisotope  $^{124}\text{I}$  ( $T_{1/2} = 4.18$  d) is both a diagnostic and a therapeutic radionuclide. It is produced at a small-sized cyclotron via the  $^{124}\text{Te}(p,n)$ -reaction and at a medium-sized cyclotron via the  $^{124}\text{Te}(d,2n)$ -process. During the period of this Report we measured excitation functions of  $^{125}\text{Te}(p,2n)^{124}\text{I}$  reaction using 98.3% enriched  $^{125}\text{Te}$  as target material. Thin target samples were prepared via electrolytic deposition of  $^{125}\text{Te}$  on Ti-backing foils. Irradiations up to  $E_p = 45$  MeV were done at Jülich and the higher energy region was investigated at Faure. From the measured data the yield and purity of  $^{124}\text{I}$  were calculated. A comparison of the three production routes of  $^{124}\text{I}$ , viz. (p,n), (d,2n) and (p,2n) processes, is given in Table 2. Because of its much higher yield, the  $^{125}\text{Te}(p,2n)$ -process appears to be very promising. Further optimising studies are under way.

Table 1. Comparison of production routes of  $^{120g}\text{I}$

Nuclear reaction	Optimum energy range [MeV]	Thick target yield of $^{120g}\text{I}$ [GBq/ $\mu\text{Ah}$ ]	Calculated impurity [%]		
			$^{120m}\text{I}$	$^{121}\text{I}$	$^{119}\text{I}$
$^{122}\text{Te}(p,3n)$	37 $\rightarrow$ 32	3.6	25	22	6
$^{120}\text{Te}(p,n)$	15 $\rightarrow$ 9	2.0	4.8	-	-
$^{120}\text{Te}(d,2n)$	13 $\rightarrow$ 9	0.37	7.5	93	-



Table 2. Comparison of production routes of  $^{124}\text{I}$ 

Nuclear reaction	Optimum energy range [MeV]	Thick target yield of $^{124}\text{I}$ [GBq/ $\mu\text{Ah}$ ]	Calculated impurity [%]	
			$^{125}\text{I}$	$^{126}\text{I}$
$^{124}\text{Te}(\text{p},\text{n})$	13 $\rightarrow$ 9	20	< 0.1	< 0.1
$^{124}\text{Te}(\text{d},2\text{n})$	16 $\rightarrow$ 6	24	a)	a)
$^{125}\text{Te}(\text{p},2\text{n})$	22 $\rightarrow$ 14	111	0.89	-

a) not determined

b) *Cross sections and yields of therapy related radioisotopes  $^{67}\text{Cu}$  and  $^{140}\text{Nd}$*

Cross section measurements relevant to the production of the radioisotope  $^{67}\text{Cu}$  ( $T_{1/2} = 61.9$  h) via the  $^{70}\text{Zn}(\text{p},\alpha)$ -process at a small-sized cyclotron (cf. last Progress Report) were completed. Although the yield is rather low, the product is of highest radionuclidic purity achieved so far (for more details cf. [9]).

The radioisotope  $^{140}\text{Nd}$  ( $T_{1/2} = 3.4$  d) can be produced via several ways. Yield measurements were done for the  $^{140}\text{Ce}(\text{}^3\text{He},3\text{n})$ -process in collaboration with the Institute of Nuclear Chemistry of the University of Mainz (F. Rösch). Further work is in progress.

c) *Compilation and evaluation of data for the production of short-lived positron emitters*

Under the auspices of the IAEA, a Co-ordinated Research Programme (CRP) on the Standardisation of Nuclear Data for the Production of Medically Important Radioisotopes has been underway for some time and has now been completed. As a participating Institute we compiled the data on the major reactions relevant to the production of the commonly used short-lived positron emitters ( $^{11}\text{C}$ ,  $^{13}\text{N}$ ,  $^{15}\text{O}$ ,  $^{18}\text{F}$ ) and performed a qualitative evaluation of the available information. On the basis of the selected data a quantitative evaluation is being done by several theory groups participating in the CRP.

# References (Publications from Jülich during the Period of the Progress Report)

- [1] R. Dóczi, S. Sudár, J. Csikai, S.M. Qaim: Excitation functions of the  $^{89}\text{Y}(n,n'\gamma)^{89\text{m}}\text{Y}$  and  $^{89}\text{Y}(n,\alpha)^{86\text{m}}\text{Rb}$  processes, *Phys. Rev. C* **58** (1998) 2577
- [2] A. Fessler, E. Wattecamps, D.L. Smith, S.M. Qaim: Excitation functions of (n,2n), (n,p), (n,np + pn + d) and (n, $\alpha$ ) reactions on isotopes of chromium, *Phys. Rev. C* **58** (1998) 996
- [3] A. Fessler, S.M. Qaim: Excitation functions of  $^{50}\text{Cr}(n,np+pn+d)^{49}\text{V}$ ,  $^{58}\text{Ni}(n,\alpha)^{55}\text{Fe}$ ,  $^{58}\text{Ni}(n,\alpha p+p\alpha)^{54}\text{Mn}$  and  $^{62}\text{Ni}(n,\alpha)^{59}\text{Fe}$  reactions, *Radiochimica Acta* **84** (1999) 1
- [4] C. Nesaraja, K.-H. Linse, S. Spellerberg, S. Sudár, A. Suhaimi, S.M. Qaim: Excitation functions of neutron induced reactions on some isotopes of zinc, gallium and germanium in the energy range of 6.2 to 12.4 MeV, *Radiochimica Acta*, in press
- [5] M. Fassbender, B. Scholten, S.M. Qaim: Radiochemical studies of (p, $^7\text{Be}$ ) reactions on biologically relevant elements in the proton energy range of 50 to 350 MeV, *Radiochimica Acta* **81** (1998) 1
- [6] M. Fassbender, Yu. N. Shubin, S.M. Qaim: Formation of activation products in interactions of medium energy protons with Na, Si, P, S, Cl, Ca and Fe, *Radiochimica Acta* **84** (1999) 59
- [7] A. Hohn, H.H. Coenen, S.M. Qaim: Nuclear data relevant to the production of  $^{120\text{g}}\text{I}$  via the  $^{120}\text{Te}(p,n)$ -process at a small-sized cyclotron, *Appl. Radiat. Isotopes* **49** (1998) 1493
- [8] B. Scholten, R.M. Lambrecht, M. Cogneau, H. Vera Ruiz, S.M. Qaim: Excitation functions for the cyclotron production of  $^{99\text{m}}\text{Tc}$  and  $^{99}\text{Mo}$ , *Appl. Radiat. Isotopes* **51** (1999) 69
- [9] S. Kastleiner, H.H. Coenen, S.M. Qaim: Possibility of production of  $^{67}\text{Cu}$  at a small-sized cyclotron via the (p, $\alpha$ )-reaction on enriched  $^{70}\text{Zn}$ , *Radiochimica Acta* **84** (1999) 107

# INSTITUT FÜR KERN- UND TEILCHENPHYSIK TECHNISCHE UNIVERSITÄT DRESDEN

## 1. Neutron and Photon Flux Spectra in an ITER Streaming Experiment\*

U. Fischer<sup>a</sup>, H. Freiesleben, W. Hansen<sup>b</sup>, D. Richter, K. Seidel, S. Unholzer

The neutronics performance of the shielding system of the International Thermonuclear Experimental Reactor (ITER) has been experimentally investigated by a compact mock-up simulating first wall, shielding blanket, vacuum vessel and toroidal field coils [1, 2]. However, the shielding capability is significantly reduced by penetrations and channels. One of the critical issues is a channel through first wall and blanket for the mechanical attachment of the blanket modules to the back-plate. To provide experimental validation of the design parameters for such a streaming path with direct sight of the d-t plasma the compact mock-up was modified by an open channel on the central axis and by a cavity at the end of the channel.

The mock-up assembled at the Frascati Neutron Generator is shown in Fig. 1. It consists of a shielding block made of alternate plates of stainless steel SS316 and the water-equivalent material PERSPEX. It is backed by a block of alternate SS316 and copper plates simulating the TF-coils. Polythene is used for shielding from room background. One series of measurements was carried out with the 14-MeV neutron source on the channel axis, and a second one with the source shifted out of the axis. Additionally, the detectors were shifted. The measurement positions are marked in Fig. 1.

A NE213 scintillation spectrometer was used for neutron spectra measurements in the energy range between about 1 MeV and 15 MeV and for flux spectra of  $\gamma$ -rays with energies  $E > 0.2$  MeV. A set of gas-filled proportional counters was applied for the lower neutron energies, down to about  $E = 30$  keV. Details of the spectrometers and the evaluation of the pulse-height spectra measured are described elsewhere [3].

---

\* Work supported by the European Fusion Technology Programme

<sup>a</sup> Forschungszentrum Karlsruhe, Institut für Neutronenphysik und Reaktortechnik

<sup>b</sup> Technische Universität Dresden, Institut für Energietechnik

For comparison with the measured flux spectra calculations with ITER design tools, the three-dimensional Monte Carlo code MCNP-4A [4] and the Fusion Evaluated Nuclear Data Library FENDL, versions 1 and 2 [5, 6], were performed. Measured fluxes in energy ranges and the ratios of calculated-to-experimental values (C/E) are presented in Table 1.

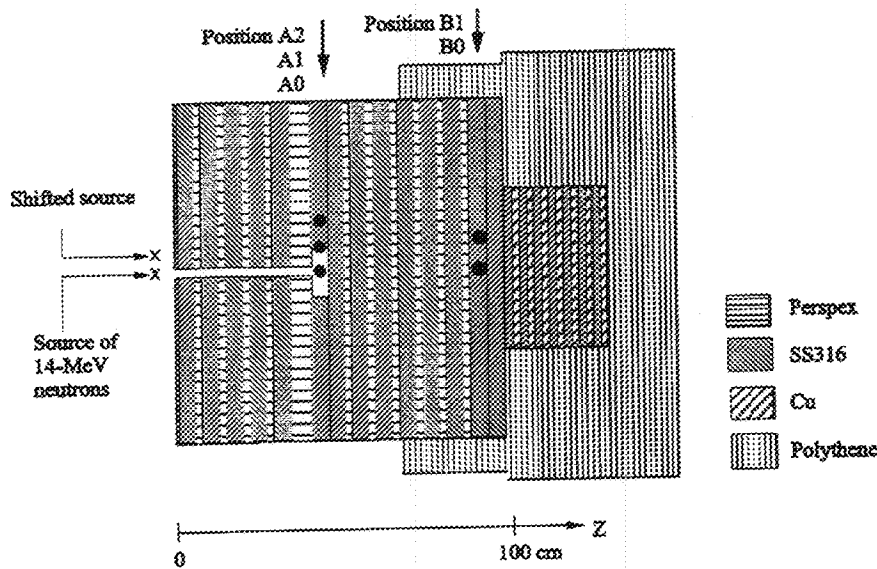


Fig. 1: Horizontal cut of the ITER mock-up assembly with streaming channel and measurement positions

The measured total neutron flux spectra in general are underestimated in the order of 10% at the back of the shielding blanket (positions A...) and in the order of 30% at the back of the vacuum vessel (positions B...). The same is true for the high energy ( $E > 10$  MeV) neutron flux, although this component is well reproduced in the compact bulk shield experiment at the shallow measuring position A. In the streaming experiment, however, there is one peculiarity for the neutron spectra obtained at the bottom of the streaming channel (Table 1: "A0 - source on axis") where the high energy ( $E > 10$  MeV) neutron flux is underestimated by as much as 20%. This behaviour requires further investigations in view of its significance to properly describe the neutron streaming through design relevant void channels and ducts.

The measured photon flux spectra can be well reproduced by the calculations. With regard to FENDL-1 and -2 data, there is no large difference in the spectra calculated

for the two locations in the ITER streaming experiment, although there is a clear trend for a better reproduction of the photon spectra with FENDL-2 at deep locations.

Table 1: Neutron and photon fluence integrals (in  $\text{cm}^{-2}$ ) measured in the ITER streaming experiment and normalized to one source neutron and calculation-to-experiment (C/E) ratios for FENDL-1 and -2 data.

	Neutron energy range				Photon energy range	
	0.1 ... 1 MeV	1 ... 5 MeV	5 ... 10 MeV	> 10 MeV	0.4 ... 1 MeV	> 1 MeV
<b>A0-source on axis</b>						
Experiment	$(3.74 \pm 0.38) \text{E-6}$	$(3.64 \pm 0.20) \text{E-6}$	$(1.04 \pm 0.10) \text{E-6}$	$(3.98 \pm 0.10) \text{E-5}$	$(0.81 \pm 0.02) \text{E-5}$	$(1.43 \pm 0.04) \text{E-5}$
FENDL-1 C/E	$1.39 \pm 0.14$	$1.32 \pm 0.08$	$1.83 \pm 0.18$	$0.78 \pm 0.02$	$0.85 \pm 0.03$	$0.79 \pm 0.03$
FENDL-2 C/E	$1.39 \pm 0.14$	$1.37 \pm 0.08$	$1.76 \pm 0.17$	$0.78 \pm 0.02$	$0.85 \pm 0.03$	$0.82 \pm 0.03$
<b>A0-source shifted</b>						
Experiment	$(2.25 \pm 0.23) \text{E-6}$	$(1.71 \pm 0.10) \text{E-6}$	$(0.42 \pm 0.04) \text{E-6}$	$(1.65 \pm 0.04) \text{E-6}$	$(4.27 \pm 0.12) \text{E-6}$	$(6.91 \pm 0.19) \text{E-6}$
FENDL-1 C/E	$1.13 \pm 0.11$	$0.96 \pm 0.06$	$1.08 \pm 0.11$	$0.84 \pm 0.03$	$0.99 \pm 0.03$	$0.99 \pm 0.03$
FENDL-2 C/E	$1.13 \pm 0.11$	$0.95 \pm 0.05$	$1.01 \pm 0.10$	$0.89 \pm 0.03$	$1.01 \pm 0.03$	$0.97 \pm 0.03$
<b>A1-source on axis</b>						
Experiment	-	$(2.10 \pm 0.12) \text{E-6}$	$(4.79 \pm 0.46) \text{E-7}$	$(1.26 \pm 0.03) \text{E-6}$	$(4.32 \pm 0.12) \text{E-6}$	$(7.16 \pm 0.20) \text{E-6}$
FENDL-1 C/E	-	$0.85 \pm 0.05$	$0.99 \pm 0.10$	$0.89 \pm 0.03$	$1.01 \pm 0.03$	$1.02 \pm 0.03$
FENDL-2 C/E	-	$0.89 \pm 0.05$	$0.99 \pm 0.10$	$0.87 \pm 0.03$	$1.06 \pm 0.03$	$1.02 \pm 0.03$
<b>A2-source on axis</b>						
Experiment	-	$(1.25 \pm 0.07) \text{E-6}$	$(2.75 \pm 0.26) \text{E-7}$	$(5.97 \pm 0.16) \text{E-7}$	$(3.13 \pm 0.09) \text{E-6}$	$(5.16 \pm 0.14) \text{E-6}$
FENDL-1 C/E	-	$0.88 \pm 0.05$	$0.97 \pm 0.09$	$0.92 \pm 0.03$	$1.00 \pm 0.03$	$0.97 \pm 0.03$
FENDL-2 C/E	-	$0.87 \pm 0.05$	$0.89 \pm 0.09$	$0.85 \pm 0.03$	$1.01 \pm 0.03$	$0.94 \pm 0.03$
<b>B0-source on axis</b>						
Experiment	$(3.26 \pm 0.33) \text{E-8}$	$(1.45 \pm 0.08) \text{E-8}$	$(0.26 \pm 0.03) \text{E-8}$	$(2.19 \pm 0.06) \text{E-8}$	$(2.52 \pm 0.07) \text{E-8}$	$(3.65 \pm 0.10) \text{E-8}$
FENDL-1 C/E	$0.72 \pm 0.07$	$0.81 \pm 0.05$	$1.07 \pm 0.11$	$0.62 \pm 0.02$	$0.77 \pm 0.03$	$0.80 \pm 0.03$
FENDL-2 C/E	$0.77 \pm 0.08$	$0.89 \pm 0.05$	$1.07 \pm 0.11$	$0.66 \pm 0.03$	$0.86 \pm 0.03$	$0.85 \pm 0.03$
<b>B0-source shifted</b>						
Experiment	$(8.32 \pm 0.84) \text{E-9}$	$(2.95 \pm 0.16) \text{E-9}$	$(0.49 \pm 0.05) \text{E-9}$	$(1.26 \pm 0.03) \text{E-9}$	$(0.68 \pm 0.02) \text{E-8}$	$(1.02 \pm 0.03) \text{E-8}$
FENDL-1 C/E	$0.73 \pm 0.07$	$0.79 \pm 0.05$	$0.90 \pm 0.09$	$0.67 \pm 0.03$	$0.85 \pm 0.03$	$0.93 \pm 0.04$
FENDL-2 C/E	$0.77 \pm 0.08$	$0.81 \pm 0.05$	$0.95 \pm 0.10$	$0.79 \pm 0.03$	$0.91 \pm 0.03$	$1.26 \pm 0.34$
<b>B1-source on axis</b>						
Experiment	-	$(1.19 \pm 0.07) \text{E-8}$	$(1.84 \pm 0.18) \text{E-9}$	$(6.71 \pm 0.17) \text{E-9}$	$(1.97 \pm 0.06) \text{E-8}$	$(2.91 \pm 0.08) \text{E-8}$
FENDL-1 C/E	-	$0.64 \pm 0.04$	$0.88 \pm 0.09$	$0.61 \pm 0.02$	$0.74 \pm 0.02$	$0.75 \pm 0.02$
FENDL-2 C/E	-	$0.71 \pm 0.04$	$0.88 \pm 0.09$	$0.67 \pm 0.02$	$0.84 \pm 0.03$	$0.94 \pm 0.14$

## References

- [1] P. Batistoni et al., Neutronics shield experiment for ITER at the Frascati neutron generator, Proceedings of the 19<sup>th</sup> Symposium on Fusion Technology, Lisbon, Portugal, 16-20 September 1996, Fusion Technology 1996, C. Varandas and F. Serra (Editors), 1997 Elsevier Science B. V., p. 233.
- [2] U. Fischer et al., Investigation of spectral neutron and gamma fluxes in a fusion reactor blanket mock-up, Progress Report on Nuclear Data Research in the Federal Republic of Germany, S. M. Qaim (Editor), NEA/NSC/DOC(97)13; INDC(GER)-043, p. 26; Jülich 1997.

- [3] H. Freiesleben et al., Measurement and analysis of neutron and photon flux spectra in the cavity, Report TU Dresden, Institut für Kern- und Teilchenphysik, TUD-IKTP/98-03, July 1998.
- [4] J. F. Briesmeister (Editor), MCNP- A general Monte Carlo n-particle transport code, Version 4A, Report LA-12625-M, Los Alamos, 1993.
- [5] S. Ganesan, P. K. Mc Laughlin, FENDL/E - Evaluated nuclear data library of neutron interaction cross-sections, photon production cross sections and photon-atom interaction cross-sections for fusion applications, Version 1.0, Report INDC(NDS)-128, IAEA Vienna, 1994.
- [6] M. Herman, A. B. Pashchenko, Extension and improvement of the FENDL library for fusion applications (FENDL-2), Report INDC(NDS)-373, IAEA Vienna, 1997.

## 2. Radioactivities induced in Fusion Reactor Structural Materials by 14 MeV Neutrons\*

R. A. Forrest<sup>a</sup>, H. Freiesleben, V. D. Kovalchuk<sup>b</sup>, D. V. Markovskij<sup>c</sup>, D. Richter, K. Seidel, V. I. Tereshkin<sup>b</sup>, S. Unholzer

Safety and environmental assessments are essential parts of fusion reactor development to ensure the attractiveness of fusion power. Safety-related investigations require among other things a reliable data base for neutron-induced radioactivity. The European Activation System (recent version EASY-97) consisting of the inventory code FISPACT and the European Activation File (EAF), is a complete tool for the calculation of activation in materials exposed to neutrons. It has been adopted for the ITER design. The aim of the present work is the experimental validation of EASY-97 for structural materials irradiated with 14 MeV neutrons. Samples of the Stainless Steel 316 (AISI 316LN(IG)), which is the structural material of ITER, of the low-activation steels MANET and F82H and of the vanadium alloys V3Ti1Si, V4Ti4Cr and V5Ti2Cr were used for benchmarks.

---

\* Work supported by the European Fusion Technology Programme and by the German Federal Ministry of Education, Science, Research and Technology

<sup>a</sup> UKAEA Fusion, Culham Science Center, Abingdon, United Kingdom

<sup>b</sup> Coordination Center "Atomsafety" Sergiev Posad, Russia

<sup>c</sup> Russian Research Center "Kurchatov Institute", Moscow, Russia

Pieces having mass of  $\leq 1$  g were irradiated at the high-intensity neutron generator SNEG-13 at Sergiev Posad with neutrons of 14.93 and 14.37 MeV mean energy. Fluences applied were of the order of  $10^{14}$  cm<sup>-2</sup>. Gamma-spectra of the samples were measured several times during decay up to about 1 year. The activities of 27 different radionuclides, identified by gamma-energies and half-life, were determined. Their half-lives range from a few hours up to 5.3 years.

For each of the measured values the activity was calculated with EASY-97, and calculated-to-experimental values (C/E) were determined.

If the uncertainty of the C/E is estimated with both the experimental errors and the calculational one, including cross section as well as half-life uncertainties, validation of EASY-97 can be stated for most of the activities. The pathways of production are analysed for all activities. Activation by protons generated in (n,p)-reactions is found to be significant.

The results were compiled in a summary report [1]. As a next step, the EAF cross sections of reactions producing activities with larger deviations of C/E from 1.0 will be compared with those of other libraries and with recent experimental data.

## Reference

- [1] K. Seidel et al., Measurement and analysis of radioactivity induced by 14 MeV neutrons in steels and vanadium alloys, Report TU Dresden, Institut für Kern- und Teilchenphysik, TUD-IKTP/99-02, April 1999.

**ABTEILUNG NUKLEARCHEMIE, UNIVERSITÄT ZU KÖLN,  
AND  
ZENTRUM FÜR STRAHLENSCHUTZ UND RADIOÖKOLOGIE,  
UNIVERSITÄT HANNOVER**

**1. Cross Section Measurements for the Production of Residual Nuclei by Medium-Energy Nucleons**

J. Protoschill<sup>1</sup>, M. Gloris<sup>1</sup>, S. Neumann<sup>1</sup>, R. Michel<sup>1</sup>, J. Kuhnhehn<sup>2</sup>, U. Herpers<sup>2</sup>, O. Jonsson<sup>3</sup>, P. Malmberg<sup>3</sup>, P.W. Kubik<sup>4</sup>, I. Leya<sup>1,5</sup>, E. Gilibert<sup>6</sup>, B. Lavielle<sup>6</sup>

High-precision cross sections for the production of residual nuclides by medium-energy proton- and neutron-induced reactions are needed for a wide variety of applications. These applications range from astrophysics over space and environmental sciences, medicine (radionuclide production, dosimetry in mixed nucleon fields, radiation therapy), accelerator technology (activation of detectors, radiation protection, on line mass separation), space and aviation technology to accelerator based nuclear waste transmutation and energy amplification.

Since it is still not possible to predict cross sections for the production of residual nuclides in nucleon-induced reactions with a precision necessary for applications [1], one has to rely on measurements. During recent years systematic investigations were performed under our collaboration to provide the data necessary for the interpretation of cosmic ray interactions with extraterrestrial matter and to satisfy some of the data needs of accelerator-driven technologies; see [2] and references therein. These efforts were continued during the reporting period and we present short summaries of our work during the last year.

---

<sup>1</sup> Zentrum für Strahlenschutz und Radioökologie, Universität Hannover, Germany

<sup>2</sup> Abteilung Nuklearchemie, Universität zu Köln, Germany

<sup>3</sup> The Svedberg Laboratory, University of Uppsala, Sweden

<sup>4</sup> Paul Scherrer Institute c/o Institut für Teilchenphysik, ETH Hönggerberg, Zürich, Switzerland

<sup>5</sup> Institut für Isotopengeologie und mineralische Rohstoffe, ETH Zürich, Zürich, Switzerland

<sup>6</sup> Centre d'Etudes Nucleaires de Bordeaux-Gradignan, France



### 1.1 Neutron-Induced Reactions

Neutron-induced reactions at medium energies are of particular importance in thick targets where secondary particles, in particular neutrons, dominate the production of residual nuclei. The assumption, which is frequently used at medium energies, that proton and neutron cross sections are equal may lead to severe errors in model calculations [3]. But, in contrast to their importance, neutron cross sections above 14 MeV are scarce. Unfortunately, there exist just a few facilities which are capable of delivering quasi-monoenergetic medium-energy neutron beams with sufficient flux densities for activation experiments.

In the past, we therefore tried to derive neutron cross sections by deconvolution techniques from residual nuclide production rates in a total of five stony and iron thick-targets which were irradiated by 600 MeV and 1.6 GeV protons in order to simulate the interactions of galactic protons with stony and iron meteoroids [4-8]. Using an energy-dependent least squares adjustment procedure [9] a set of neutron excitation functions for about 500 target-product combinations from their thresholds up to 900 MeV was derived [10,11]. On the basis of our cross section data base for proton- and neutron-induced reactions and of Monte Carlo simulations of the galactic cosmic ray primary and secondary spectra inside meteoroids, we were able to establish model calculations for cosmogenic nuclide production rates in extraterrestrial matter, such as stony and iron meteoroids and lunar surface materials, with an accuracy better than 10 % for production rates and better than 3 % for production rate ratios [12-14].

The target element coverage and the respective cross section data base for the cosmochemical applications does just partially satisfy the data needs of accelerator-driven technologies. Therefore, we extended our investigations to activation experiments with quasi-monoenergetic medium-energy neutron beams. Experiments were first performed at the neutron beam line [15] of the The Svedberg Laboratory (TSL) at Uppsala (Sweden). A special facility was installed [16] which allows for parasitic irradiation experiments with neutron energies between 70 MeV and 180 MeV. In a series of ongoing irradiations, the target elements C, O, Al, Mg, Si, Fe, Co, Ni, Cu, Ag, Te, Pb are investigated. Direct measurements of the neutron peak fluence were carried out by means of thin-film breakdown counters [17] in collaboration with the V.G. Khlopin

Radium Institute/St. Petersburg (Russia).

In addition, irradiation experiments were performed in reference neutron fields [18] at the neutron beam line of the Universite Catholique de Louvain (UCL) at Louvain-la-Neuve (Belgium). Three experiments with quasi-monoenergetic neutron beams were carried out with peak energies of 33.7 MeV, 46.0 MeV, and 60.6 MeV. Absolute data for the neutron flux density spectrum in the energy range from 3 MeV up to the peak energies were taken by using different measurement techniques [18] from the collaborating group of the Physikalisch-Technische Bundesanstalt/Braunschweig (Germany).

In all these experiments, residual nuclides are measured by off-line  $\gamma$ -spectrometry. Data were obtained for nuclides with half-lives between 20 minutes ( $^{11}\text{C}$ ) and five years ( $^{60}\text{Co}$ ). Later on, measurements of long-lived products are planned via accelerator mass spectrometry using the ETH/PSI AMS facility in Zürich (Switzerland). Up to now only spectrum-weighted production cross sections can be given [19] since the evaluation of point-wise cross section, which also in this case can only be performed by deconvolution techniques, will be done after a whole series of irradiation experiment with energies between 30 and 180 MeV.

## 1.2 Proton-Induced Reactions

Investigations of residual nuclide production by proton-induced reactions were systematically continued. The actual work in the reporting period was related to further improvement of the data base for cosmogenic nuclide production and to the data needs of accelerator-driven technologies.

With respect to cosmogenic nuclides, new cross sections were measured for the production of Kr-isotopes from Rb, Sr, Y, and Zr in the energy range from some tens of MeV up to 1.6 GeV [20] as well as thick-target production rates from the above mentioned simulation experiments [6-9]. Thus, a comprehensive and consistent data base of proton and neutron cross sections was established which allows for the first time reliable model calculations of cosmogenic krypton in extraterrestrial matter [21]. Moreover, as a by-product excitation functions for the production of 31 short-lived

nuclides were measured by  $\gamma$ -spectrometry prior to mass spectrometry [20].

Also with respect to cosmogenic nuclides, new cross section measurements were performed for the proton-induced production of stable helium and neon isotopes from magnesium, aluminum and silicon [22]. The new data provide the basis for improved model calculations of  $^3\text{He}/^{21}\text{Ne}$  and  $^{22}\text{Ne}/^{21}\text{Ne}$  production rate ratios in meteoroids which are widely used in meteoritics as indicators of the size of an irradiated body and of the depth of a sample in it [14]. Ongoing work is dedicated to improve the cross section data base for the cosmogenic nuclides  $^{41}\text{Ca}$  ( $T_{1/2} = 104 \text{ ka}$ ),  $^{53}\text{Mn}$  ( $T_{1/2} = 3.7 \text{ Ma}$ ),  $^{60}\text{Fe}$  ( $T_{1/2} = 1.49 \text{ Ma}$ ), and  $^{129}\text{I}$  ( $T_{1/2} = 15.7 \text{ Ma}$ ).

With respect to accelerator-driven technologies, measurements of targets and evaluation of thin-target experiments performed at Laboratoire National Saturne at Saclay (France) and at TSL for proton energies between 70 MeV and 2.6 GeV were continued. These elements covered the target elements Mo, Ag, In, Te, Ta, W, Re, Ir, Pb, and Bi in addition to those investigated earlier [2]. In order to investigate the same target elements for proton energies below 70 MeV, experiments at the Paul Scherrer Institute (PSI) at Villigen (Switzerland) are going on.

For the target element lead, now final data are being published covering about 2000 individual cross sections for 127 reactions for proton-energies between 64.8 MeV and 2.6 GeV [23,24]. The excitation functions exhibit clearly distinguishable reaction modes like multi-fragmentation, three different types of asymmetric and symmetric fission, and deep spallation. Together with the new data, a comprehensive comparison with theoretical predictions by the LAHET code system are presented. Together with earlier model exercises, e.g. [1], this comparison demonstrates the necessity for further improvements of models and codes if medium-energy activation cross sections for applications shall be reliably predicted by theory. A comparison of different intranuclear cascade/evaporation models and a detailed parameter study will be published together with the final results obtained for the target element bismuth (in preparation).

Here, we report on new results for the target element tungsten. Excitation functions were measured for the production of 61 radionuclides in the energy range from 70 MeV to 2.6 GeV comprising about 950 new cross sections. Fig. 1 gives some

examples. The dependence of cross sections on product mass numbers also allows to distinguish between reaction modes such as spallation, fission and fragmentation for the target element tungsten (Fig. 2). But, in contrast to lead, just one fission mode can be observed. Neither asymmetric fission nor a fission mode leading to neutron-rich products with thresholds well below 100 MeV and plateau-like excitation functions are to be seen. Among all fission products, the excitation function for the production of  $^{84}\text{Rb}$  (Fig. 1) has the lowest slope of the excitation function with increasing proton energy. For many reactions the excitation functions are already complete. But, for products near the target, the experiments at PSI will be needed to get complete excitation functions.

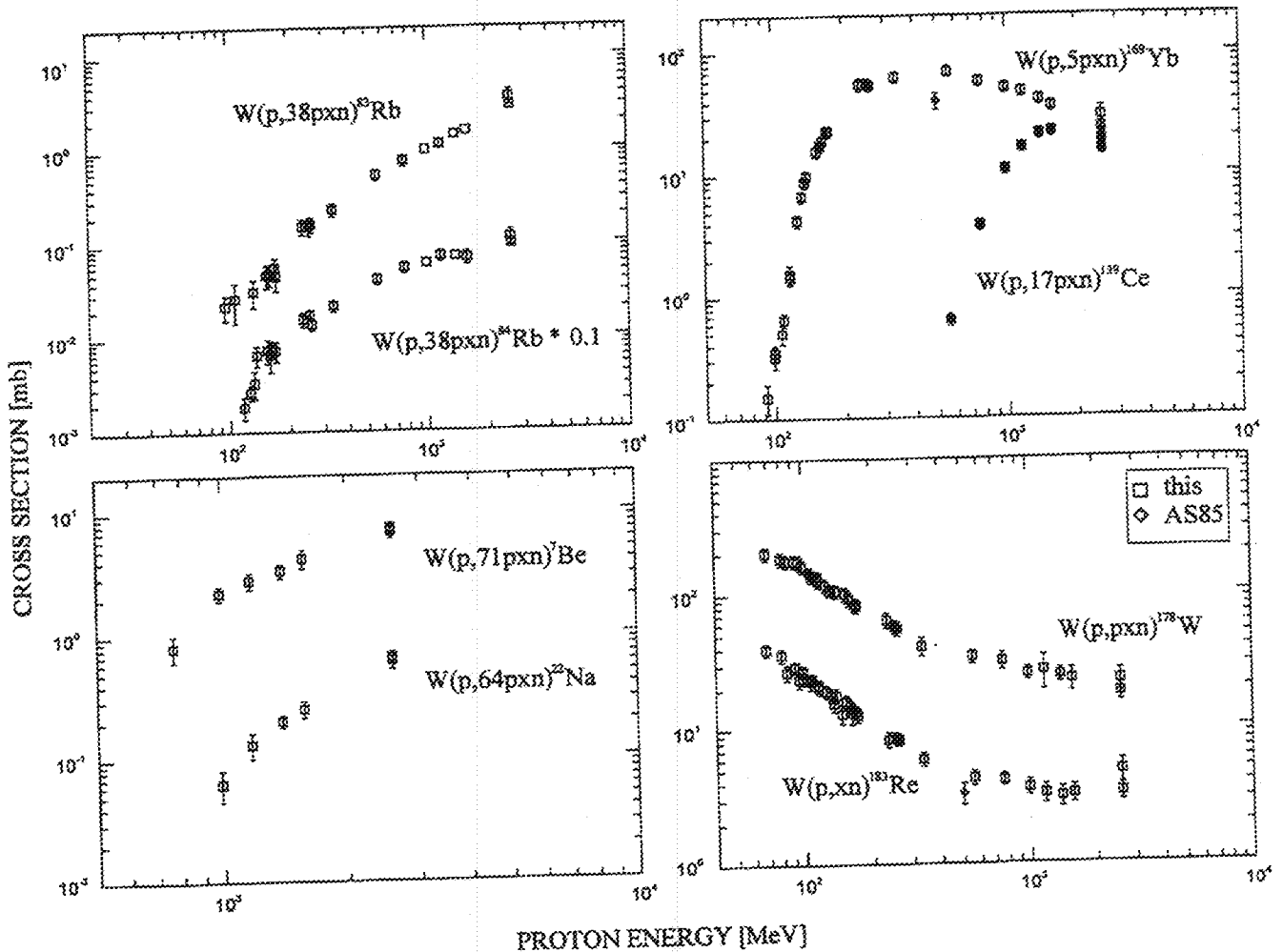


Fig. 1 Examples of excitation functions measured for the production of residual nuclides by proton-induced reactions on tungsten. There is just one earlier work below 10 GeV [25] dealing with proton-induced radionuclide production from tungsten.

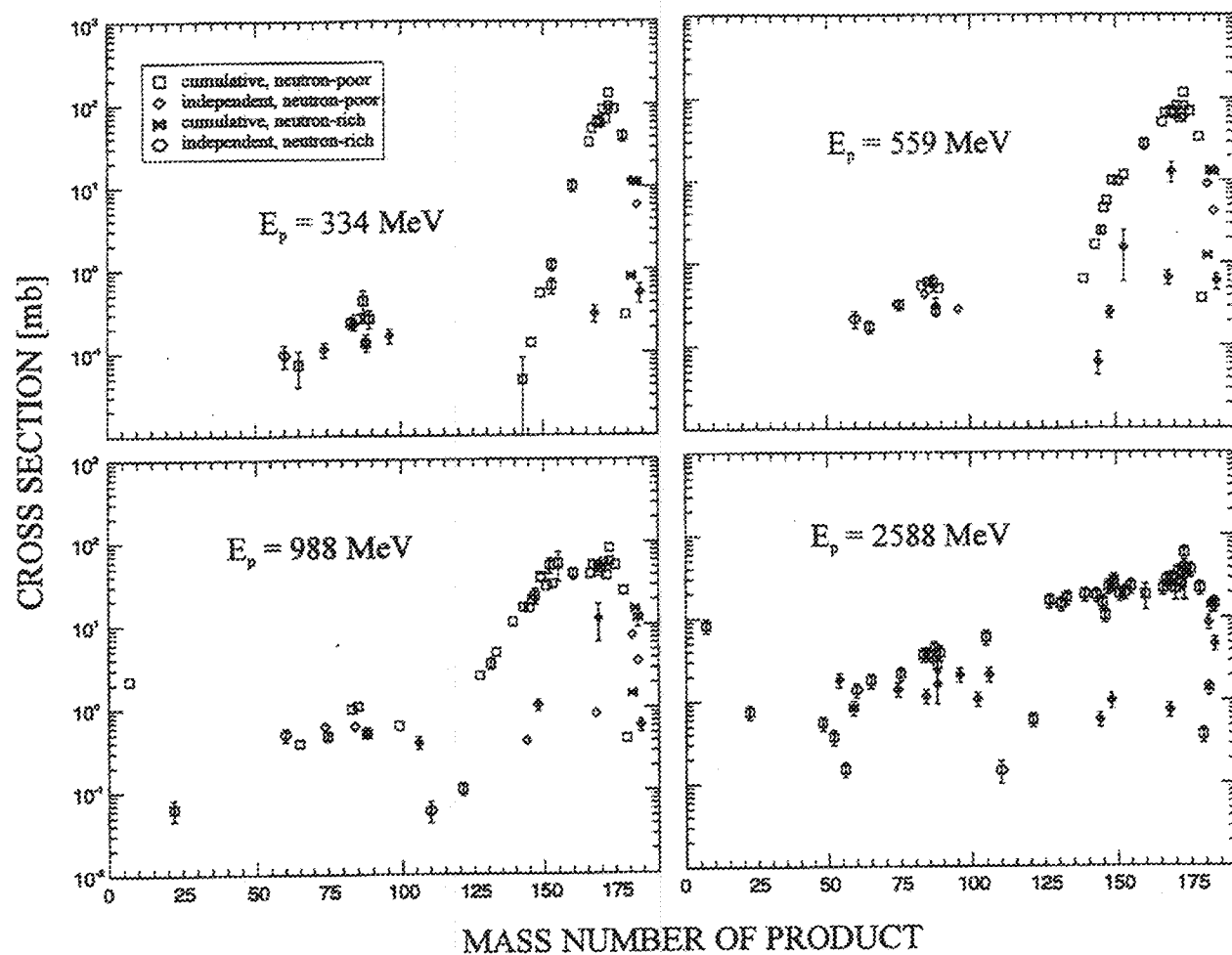


Fig. 2 Measured cross sections in tungsten for different proton energies  $E_p$  in dependence of product nuclide mass number. Different symbols indicate whether the cross sections are cumulative or independent ones and whether the products are from the neutron-rich or neutron-poor side of the valley of stability.

### Acknowledgement

The authors thank the authorities of LNS, PSI, UCL and TSL for the beam-time and the accelerator staffs for their cooperation and assistance. This work was supported partially by the Deutsche Forschungsgemeinschaft, Bonn, by the Swiss National Science Foundation, Bern, and by the CEC in the Human Capital and Mobility Program and in the Concerted Action "Lead for Transmutation".

## References

- [1] R. Michel, P. Nagel, International Codes and Model Comparison for Intermediate Energy Activation Yields, NSC/ DOC (97)-1, OECD/NEA, Paris, 1997.
- [2] R. Michel et al., Cross sections for the production of residual nuclides by low- and medium-energy protons from the target elements C, N, O, Mg, Al, Si, Ca, Ti, Mn, Fe, Co, Ni, Cu, Sr, Y, Zr, Nb, Ba and Au, Nucl. Instr. Meth. Phys. Res. **B129** (1997) 153
- [3] R. Michel, M. Gloris, S. Neumann, I. Leya, Neutron cross sections for physical model calculations of cosmogenic nuclide production rates, Meteoritics & Planetary Science **33** No. 4 Supplement (1998) A108
- [4] R. Michel, P. Dragovitsch, P. Englert, F. Peiffer, R. Stück, S. Theis, F. Bege- mann, H. Weber, P. Signer, R. Wieler, D. Filges, P. Cloth, On the depth-depen- dence of spallation reactions in a spherical thick diorite target homogenously irradiated by 600 MeV protons. Simulation of production of cosmogenic nuclides in small meteorites, Nucl. Instr. Meth. Phys. Res. **B16** (1986) 61 - 82
- [5] R. Michel, F. Peiffer, S. Theis, F. Bege- mann, H. Weber, P. Signer, R. Wieler, P. Cloth, P. Dragovitsch, D. Filges, P. Englert, Production of stable and radioactive nuclides in thick stony targets ( $R = 15$  and  $25$  cm) isotropically irradiated with 600 MeV protons. Simulation of production of cosmogenic nuclides in mete- orites, Nucl. Instr. Meth. Phys. Res. **B42** (1989) 76 - 100
- [6] R. Michel, M. Lüpke, U. Herpers, D. Filges, P. Dragovitsch, W. Wölfli, B. Dittrich, H.J. Hofmann, Simulation of the interactions of galactic cosmic ray protons by isotropic irradiation of a thick stony target with 1.6 GeV protons, J. Radioanal. Nucl. Chem. **169** (1993) 13-25
- [7] R. Michel, H.-J. Lange, M. Lüpke, U. Herpers, R. Rösel, M. Suter, B. Dittrich- Hannen, P.W. Kubik, D. Filges, P. Cloth, Simulation and modeling of the inter- action of galactic protons with stony meteoroids, Planetary and Space Science **43** (1995) 557-572
- [8] I. Leya, H.-J. Lange, M. Lüpke, U. Neupert, R. Daunke, O. Fanenbruck, R. Michel, R. Rösel, B. Meltzow, T. Schiek, F. Sudbrock, U. Herpers, D. Filges, G. Bonani, B. Dittrich-Hannen, M. Suter, P.W. Kubik, H.-A. Synal, Simulation of the interaction of gcr protons with meteoroids - on the production of radio- nuclides in thick gabbro and steel targets irradiated isotropically with 1.6 GeV protons -, Meteoritics & Planetary Science, submitted 1998.
- [9] M. Matzke, Unfolding by least-squares methods: SAND-II, STAY'SL, Proc. 3rd ASTM-Euratom Symposium on Reactor Dosimetry, Ispra, 1.-5.10.1979, pp. 721 - 731 (1979).
- [10] I. Leya, Model calculations for the description of the interaction of galactic cosmic particle rays with stony and iron-meteorites - thin-target irradiations and thick-target experiments (translated title), Ph. D. Thesis, University Hanover (1997).

- [11] I. Leya, R. Michel, Determination of neutron cross sections for nuclide production at intermediate energies by deconvolution of thick-target production rates, in: G. Reffo, A. Ventura, C. Grandi (eds.), Proc. Int. Conf. Nuclear Data for Science and Technology, Trieste, 19-24 May 1997, IPS Conf. Proc. 59 Bologna (1997) 1463
- [12] R. Michel, I. Leya, L. Borges, Nucl. Instr. Meth. in Phys. Res. **B113** (1996) 434
- [13] R. Michel, S. Neumann, Interpretation of cosmogenic nuclides in meteorites on the basis of accelerator experiments and physical model calculations, Proc. Int. Conf. Isotopes in the Solar System, 50th Anniversary of PRL Ahmedabad, Proc. Indian Acad. Sci. (Earth Planet. Sci.) **107** No. 4 (1998) 441 - 457
- [14] I. Leya, H.-J. Lange, S. Neumann, R. Wieler, R. Michel, The production of cosmogenic nuclides in stony meteoroids by galactic cosmic ray particles, Meteoritics & Planetary Science, submitted 1999.
- [15] H. Condé, S. Hulqvist, N. Olsson, T. Rönnqvist, R. Zorro, J. Blomgren, G. Tibell, A. Hakansson, O. Jonsson, A. Lindholm, L. Nilsson, P.-U. Renberg, A. Brockstedt, P. Ekström, M. Österlundt, F.P. Brady, Z. Szefflinski, A facility for studies of neutron-induced reactions in the 50 - 200 MeV range, Nucl. Instr. Meth. Phys. Res. **A292** (1990) 121 - 128
- [16] S. Neumann, R. Michel, F. Sudbrock, U. Herpers, P. Malmberg, O. Jonsson, B. Holmqvist, H. Conde, P.W. Kubik, M. Suter, A new facility at the The Svedberg Laboratory for activation experiments with medium energy neutrons, in: G. Reffo, A. Ventura, C. Grandi (eds.), Proc. Int. Conf. Nuclear Data for Science and Technology, Trieste, 19-24 May 1997, IPS Conf. Proc. 59 Bologna (1997) 379
- [17] V.P. Eismont, A.I. Obukhov, A. V. Prokofyev, A.N. Smirnov, Relative and absolute neutron-induced fission cross sections of  $^{208}\text{Pb}$ ,  $^{209}\text{Bi}$ , and  $^{238}\text{U}$  in the intermediate energy region, Phys. Rev. **C53** (1996) 2911
- [18] H. Schumacher, H.J. Brede, V. Dangendorf, M. Kuhfuss, J.P. Meulders, W.D. Newhauser, R. Noite, U.J. Schrewe, Quasi-monoenergetic reference neutron beams with energies from 25 MeV to 70 MeV, in: G. Reffo, A. Ventura, C. Grandi (eds.), Proc. Int. Conf. Nuclear Data for Science and Technology, Trieste, 19-24 May 1997, IPS Conf. Proc. 59 Bologna (1997) 1534
- [19] S. Neumann, Activation experiments with neutrons of medium energies and production of cosmogenic nuclides in extraterrestrial matter (translated title), Ph. D. thesis, University Hanover (1998).
- [20] E. Gilabert, B. Lavielle, S. Neumann, M. Gloris, R. Michel, Th. Schiekkel, F. Sudbrock, U. Herpers, Cross sections for the proton-induced production of krypton isotopes from Rb, Sr, Y, and Zr for energies up to 1600 MeV, Nucl. Instr. Meth. Phys. Res. **B145** (1998) 293 - 319
- [21] E. Gilabert, B. Lavielle, Th. Schiekkel, U. Herpers, S. Neumann, I. Leya, R. Michel, Measurements and modeling the production of krypton and xenon in a simulation experiment of an artificial iron meteoroid: application to the chondrite Knyahinya, Meteoritics & Planetary Science **32** (1997) A47

- [22] I. Leya, H. Busemann, H. Baur, R. Wieler, M. Gloris, S. Neumann, R. Michel, F. Sudbrock, U. Herpers, Cross sections for the proton-induced production of He and Ne isotopes from magnesium, aluminum, and silicon, Nucl. Instr. Meth. Phys. Res. **B145** (1998) 449 – 458
- [23] M. Gloris, R. Michel, F. Sudbrock, U. Herpers, P. Malmborg, B. Holmqvist, Proton-induced production of residual nuclei in lead at intermediate energies, Nucl. Instr. Meth. Phys. Res. A in press 1999.
- [24] M. Gloris, Proton-induced production of residual nuclei in heavy elements at medium energies (translated title), Ph. D. Thesis, University Hanover (1998).
- [25] M. Asano, S. Mori, M. Noguchi, M. Gakano, K. Katoh, K. Kondo, Spallation and fission yields in the interaction of tantalum, tungsten and gold with 500 MeV protons J. Phys. Soc. Japan **54** (1985) 3734 - 3741



# INSTITUT FÜR KERNCHEMIE UNIVERSITÄT MAINZ

## Shell Effects in the Very Asymmetric Fission of $^{242m}\text{Am}$ by Thermal Neutrons

I. Tsekhanovitch<sup>1</sup>, H. O. Denschlag, M. Davi, Z. Büyükmumcu<sup>2</sup>, M. Wöstheinrich<sup>3</sup>,  
 F. Gönnerwein<sup>3</sup>, S. Oberstedt<sup>4</sup>

Measurements of fission product yields were carried out for the compound nucleus  $^{243}\text{Am}^*$  at the mass separator for unsloved fission fragments Lohengrin in Grenoble in the region of very light masses. The mass separated fission products were detected in an ionisation chamber with split anode. The specific energy loss of the fragments measured in the first part of the ionisation chamber allows to identify the nuclear charge of the fission products. The absolute yields obtained in the mass region studied are shown in Fig. 1.

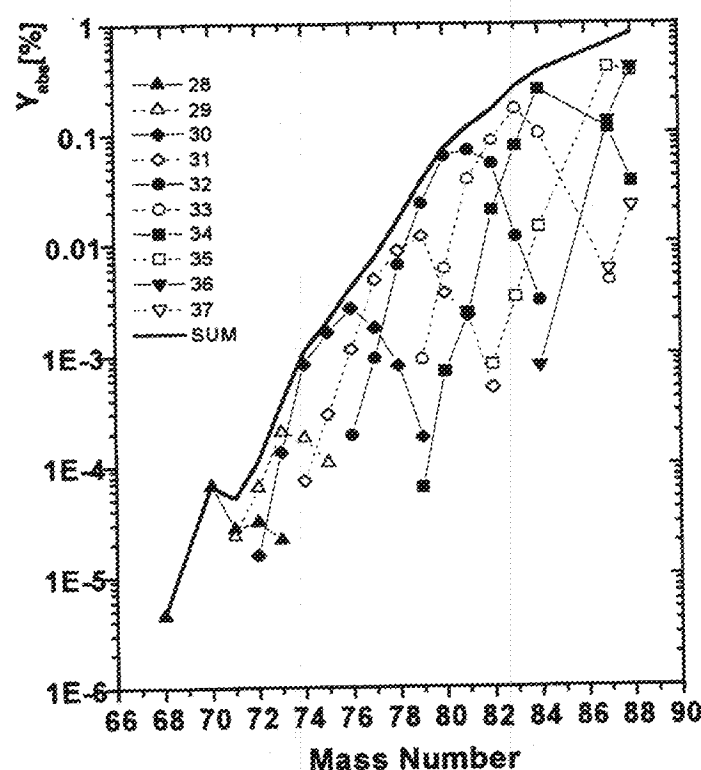


Fig. 1: Absolute yields (%) of single nuclides (atomic numbers (Z) in the insert).  
 The drawn-out line represents the chain yields.

<sup>1</sup>Radiation Physics and Chemistry Problems Institute, 220109 Minsk, Belarus

<sup>2</sup>Middle East Technical University, 06531 Ankara, Turkey

<sup>3</sup>Physikalisches Institut, Universität Tübingen

<sup>4</sup>Institut Laue-Langevin, Grenoble, France

Fission products with even  $Z$  are shown as full data points and drawn-out lines; those with odd  $Z$  are given by open symbols and dashed lines. The maxima of the drawn out lines approach more closely the line of chain yields, demonstrating again an odd-even effect in the odd- $Z$  nucleus  $\text{Am}$  ( $Z = 95$ ) that has been discussed in more detail in last year's contribution of this laboratory [1] on the basis of a more limited data base.

A point of specific interest is the fine structure at mass  $A = 70$  that has been observed also in the thermal neutron induced fission reactions of  $^{235}\text{U}$  (by Sida et al. [2]), and of  $^{239}\text{Pu}$  [3], as well as  $^{249}\text{Cf}$  [4] (by our group). The present case of  $\text{Am}$ , however, shows the first occurrence of this fine structure in the fission of an odd- $Z$  nucleus. In all cases observed, the fission products of mass 70 consist practically only of nickel ( $> 90\%$ ). Nickel has the atomic number  $Z = 28$  that represents a shell closure. Therefore the fine structure is interpreted as a shell effect. Also here it appears that the existence of an unpaired proton in the ground state of  $\text{Am}$  does not induce an increased excitation at scission.

A detailed inspection of Fig. 1 reveals a weak kink in the mass yield curve at  $A = 80$ . Since the change of the yield values by several orders of magnitude brings about a compression of the Y-axis, Fig. 2 shows the mass region from  $A = 74$  to 84 in more detail. In addition, Fig. 2 shows mass yields of other fission reactions, as far as available in this mass region.

It appears that all the mass yield curves measured show a kink at mass 80. (For  $\text{Cf}$  the kink is a bit weaker, presumably due to the higher fissility and seems to lie rather at  $A = 79$ ). We interpret this observation as a confirmation of the theoretical results of Brosa et al. [6], indicating that, at the variation of the mass of the compound nuclei, both light and heavy sphere of the dumbbell-shaped scission configuration remain unchanged and that the difference in mass appears predominantly in the neck. On these grounds the probability for fragments smaller than 80 should be clearly diminished – in agreement with the corresponding findings for mass 132 among the heavy fragments.

The resulting constant mass of the light sphere of  $A = 80$  is in agreement with the observation that ternary fragments (originating from the neck), show a systematic increase of heavier particles with increasing mass of the compound nucleus [7].

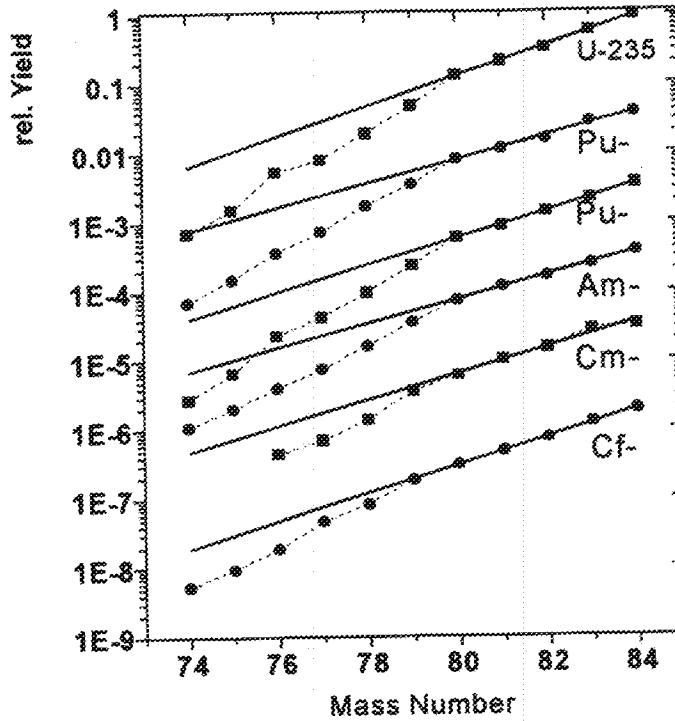


Fig. 2: Section of the mass yield curves of various nuclides after fission by thermal neutrons ( $^{235}\text{U}$  [2],  $^{239}\text{Pu}$  [3],  $^{241}\text{Pu}$  [5],  $^{242\text{m}}\text{Am}$  [this work],  $^{245}\text{Cm}$  [5] and  $^{249}\text{Cf}$  [4]). In order to enhance the visibility of the change in slope the data in the mass range  $A = 80$  to  $84$  have been fitted by straight lines (in this logarithmic display). For reasons of clarity the single curves shown are displaced relative to each other by a factor of 10.

The observation at  $A = 80$  has to be seen in connection with the fine structure at  $A=70$  ( $Z = 28$ ). It seems reasonable that the double shell closure in the light fragment, which would occur at  $^{78}\text{Ni}$  ( $A = 78$ ,  $Z = 28$ ,  $N = 50$ ), cannot be realised because its charge density is too far off the charge density of the compound nuclei ( $Z_{\text{UCD}}$ ). Therefore the double shell closure is accomplished in two steps: A fragment of mass 80 (according to the present measurements for  $^{243}\text{Am}^*$ ) contains on the average 32 protons and, in consequence, 48 neutrons (i.e.  $N \approx 49$  prior to prompt neutron emission). One can imagine the light sphere to be built like an avocado: a hard inner core with  $Z = 28$ / $N = 42$  is surrounded by further nucleons that establish  $N \approx 50$ . The structures of both heavy and light spheres have a remarkable stability, so that they remain essentially unchanged for a mass range of the compound nuclei from  $A_F = 234$  to 250.

## References

- [1] M. Davi, H. O. Denschlag, H. R. Faust, F. Gönnerwein, S. Oberstedt, I. Tsekhanovitch, M. Wöstheinrich: Odd-Even Effects in the Fission of Odd-Z Nuclides; in S.M. Qaim (Ed.) Progress Report on Nuclear Data Research in the Federal Republic of Germany, Report NEA/NSC/DOC(98)7; INDC(Ger)-044; Jül-3550
- [2] J.L. Sida, P. Armbruster, M. Bernas, J.P. Bocquet, R. Brissot, H. R. Faust, Nucl. Phys. **A502** (1989) 233c
- [3] W. Ditz, Dissertation, Mainz (1991)
- [4] R. Hentzschel, H. R. Faust, H.O. Denschlag, B. D. Wilkins, J. Gindler Nucl. Phys. **A571** (1994) 427
- [5] T. Friedrichs, H. Faust, G. Fioni, M. Groß, U. Köster, F. Münnich, S. Oberstedt, in: Nuclear Fission and Fission Product Spectroscopy, AIP Conference Proceedings **447** (1998) 231 and Th. Friedrichs, Dissertation, Braunschweig (1998)
- [6] U. Brosa, S. Großmann, A. Müller, Physics Reports **197** (1990) 167
- [7] M. Wöstheinrich, R. Pfister, F. Gönnerwein, H. O. Denschlag, H. Faust, S. Oberstedt, in: Nuclear Fission and Fission Product Spectroscopy, AIP Conference Proceedings **447** (1998) 330

**PHYSIK DEPARTMENT DER  
TECHNISCHEN UNIVERSITÄT MÜNCHEN  
FRM-REAKTORSTATION GARCHING**

**Theoretical Evaluation of Neutron-nucleus Scattering Parameters from Experimental Data in the  $6 \leq A < 60$  Mass Region**

A. Aleksejevs\*, S. Barkanova\*, J. Tambergs\*, T. Krasta\*, W. Waschkowski, K. Knopf

Systematic calculations of the neutron-nucleus scattering parameters at several neutron energies  $E_i < 2$  keV have been performed for 37 isotopes ( ${}^6\text{Li}$ , ...  ${}^{59}\text{Co}$ ) in the mass region of  $6 \leq A < 60$ , using the large compilation of experimental neutron-nucleus scattering data obtained in Garching. In the first stage of these calculations, the  $s$ -wave potential scattering radius  $R'$ , the scattering lengths  $b_{\text{coh}}$ ,  $b_{\text{tr}}$ , and the bound state parameters ( $E_b$ ,  $\Gamma_{\text{tr}}$ ,  $g\Gamma_{\text{a}}^0$ ) have been calculated for each isotope, employing the general least squares fit (GLSQF) for the experimental and the corresponding theoretical values of the total neutron-nucleus cross sections  $\sigma_{\text{tot}}^{\text{exp}}(E_i)$  at several energies  $E_i$ , absorption cross sections  $\sigma_{\text{abs}}(E_0)$  and of the coherent scattering lengths  $b_{\text{coh}}$ . The theoretical expressions for these parameters were deduced on the basis of the usual  $S$ -matrix formalism with no assumption about the particular shape of the optical model potential. In the second stage of our calculations, the spherical Fiedeldey-Frahn optical potential was employed for the pure theoretical description of the above mentioned neutron-nucleus scattering characteristics. The results obtained have been analyzed and compared with the values deduced from measurements. (For detailed results cf. Z. Naturforsch. 53a (1998) 855 – 862)

---

\* Nuclear Research Center, 31 Miera Str., LV-2169, Salaspils, Latvia

# PHYSIKALISCH-TECHNISCHE BUNDESANSTALT BRAUNSCHWEIG

## 1. Evaluation of a 'Best Set' of Average Cross Section Measurements in the $^{235}\text{U}(n_{\text{th}},f)$ Neutron Field

W. Mannhart

Compared with the neutron spectrum of spontaneous fission of  $^{252}\text{Cf}(sf)$ , for which a detailed evaluation exists (see Tape 106 of ENDF/B-VI), present knowledge of the technically important fission neutron spectrum of  $^{235}\text{U}(n_{\text{th}},f)$  is less well established. Recent attempts to recalculate the spectral shape of the  $^{235}\text{U}(n_{\text{th}},f)$  fission neutron spectrum on the basis of refined theoretical models [1] have motivated the present work.

The last systematic evaluation of average cross sections measured in the thermal-neutron induced fission neutron field of  $^{235}\text{U}$  dates back to 1976 [2]. As details are missing, the evaluation was considered unsuitable for a simple updating. The whole database available has therefore been reanalysed for a new evaluation with the aim of using the integral data in future steps for the verification and a possible adjustment of the spectral shape of the  $^{235}\text{U}(n_{\text{th}},f)$  neutron field.

The present evaluation is based on 38 experiments, mainly taken from the EXFOR database, which have remained after a preselection process excluding experiments with an improper documentation or performed without sufficiently clean experimental conditions. The number of available experiments includes 15 experiments performed after 1976. The present evaluation is based on a total of 200 data and comprises the measurement of 30 different neutron reactions. Only 4 of the 200 data were obtained in absolute measurements. Two of these absolute measurements were based on a transfer between the  $^{252}\text{Cf}$  and the  $^{235}\text{U}$  neutron field. The large remainder were ratio measurements performed relative to various neutron monitor reactions. The dominating ratio measurements define a strongly dependent system of data which requires a simultaneous evaluation procedure.

Before the evaluation process, for each experiment the radioactive decay data used in the measurement of the individual neutron reactions were checked and updated to the most recent values (current issues of the Nuclear Data Sheets). Then the quoted values were restored to the original ratios. Obviously wrong and inconsistent values of 25 of the experimental data were rejected. In a few cases the quoted uncertainties were modified according to the documentation on hand. After these steps the evaluation was performed using a generalized least-squares code which linked the ratio measurements to the absolute ones. The evaluation resulted in a value of chi-square per degree of freedom of 0.71 and indicated no serious inconsistencies among the available data of the 30 different neutron reactions. The result is given in Table 1 and compared with two previous evaluations [2,3]. The sequence of the reactions is arranged according to increasing energy response ranges in the neutron field. All reactions together cover an energy range between 0.2 and 18 MeV.

As an additional check of the internal consistency of the present result, the data obtained are compared with those which resulted from a similar evaluation of integral measurements performed in the  $^{252}\text{Cf}(\text{sf})$  neutron field [4]. The ratio of the evaluated average cross sections in the  $^{252}\text{Cf}(\text{sf})$  neutron field relative to that obtained for the  $^{235}\text{U}(\text{n}_{\text{th}},\text{f})$  neutron field was formed for each individual neutron reaction and plotted as a function of the mean energy  $E(50\%)$  of the energy response valid in the neutron field of spontaneous fission of  $^{252}\text{Cf}$ . The result is shown in Fig. 1, including the combined uncertainties (one standard deviation). A polynomial of the 2<sup>nd</sup> order has been fitted to the data. The increase of the ratio to higher neutron energies reflects the somewhat harder neutron spectrum of  $^{252}\text{Cf}(\text{sf})$ . Within the given uncertainties none of the formed ratios deviates substantially from the fitted curve with the exception of the value of the  $^{63}\text{Cu}(\text{n},2\text{n})$  reaction which has been excluded from the fitting procedure. This perfect agreement is a sound confirmation that the present evaluation is free of unknown inconsistencies between the integral responses of the various neutron reactions. The value of the ratio of the  $^{63}\text{Cu}(\text{n},2\text{n})$  reaction requires further investigation. At present it is not understood if the inconsistency results from the  $^{252}\text{Cf}(\text{sf})$  or the  $^{235}\text{U}(\text{n}_{\text{th}},\text{f})$  data.

Table 1: Evaluated experimental data of  $\langle \sigma \rangle$  in the  $^{235}\text{U}(n_{\text{th}}, f)$  neutron field

Reaction	Present work $\langle \sigma \rangle$ in mb	Fabry (1976) $\langle \sigma \rangle$ in mb	Calamand (1974) $\langle \sigma \rangle$ in mb
U-235(n,f)	1219 $\pm$ 14	1203 $\pm$ 30	1250 $\pm$ 70
Pu-239(n,f)	1835 $\pm$ 30	1811 $\pm$ 60	
Np-237(n,f)	1353 $\pm$ 24	1312 $\pm$ 50	
In-115(n,n')In-115m	188.2 $\pm$ 2.3	189 $\pm$ 8	188 $\pm$ 11
U-238(n,f)	309.9 $\pm$ 3.5	305 $\pm$ 10	328 $\pm$ 10
Ti-47(n,p)Sc-47	17.90 $\pm$ 0.36	19.0 $\pm$ 1.4	20.0 $\pm$ 2.3
S-32(n,p)P-32	69.30 $\pm$ 1.35	66.8 $\pm$ 3.7	69 $\pm$ 4
Ni-58(n,p)Co-58m+g	108.5 $\pm$ 1.4	108.5 $\pm$ 5.4	113 $\pm$ 7
Zn-64(n,p)Cu-64	35.50 $\pm$ 1.07	29.9 $\pm$ 1.6	31.0 $\pm$ 2.3
Fe-54(n,p)Mn-54	79.96 $\pm$ 1.10	79.7 $\pm$ 4.9	82.5 $\pm$ 5.0
Co-59(n,p)Fe-59	1.401 $\pm$ 0.033		1.42 $\pm$ 0.14
Al-27(n,p)Mg-27	3.914 $\pm$ 0.070	3.86 $\pm$ 0.25	4.00 $\pm$ 0.45
Ti-46(n,p)Sc-46m+g	11.55 $\pm$ 0.20	11.80 $\pm$ 0.75	12.5 $\pm$ 0.9
V-51(n,p)Ti-51	(4.980 $\pm$ 0.130) E-1		(8.7 $\pm$ 1.1) E-1
Cu-63(n, $\alpha$ )Co-60	(4.935 $\pm$ 0.242) E-1	(5.00 $\pm$ 0.56) E-1	(5.0 $\pm$ 0.6) E-1
Fe-56(n,p)Mn-56	1.083 $\pm$ 0.017	1.035 $\pm$ 0.075	1.07 $\pm$ 0.08
Mg-24(n,p)Na-24	1.455 $\pm$ 0.023	1.480 $\pm$ 0.082	1.53 $\pm$ 0.09
Co-59(n, $\alpha$ )Mn-56	(1.568 $\pm$ 0.035) E-1	(1.43 $\pm$ 0.10) E-1	(1.56 $\pm$ 0.09) E-1
Ti-48(n,p)Sc-48	(3.007 $\pm$ 0.054) E-1	(3.00 $\pm$ 0.18) E-1	(3.15 $\pm$ 0.27) E-1
Al-27(n, $\alpha$ )Na-24	(7.031 $\pm$ 0.090) E-1	(7.05 $\pm$ 0.40) E-1	(7.25 $\pm$ 0.45) E-1
V-51(n, $\alpha$ )Sc-48	(2.438 $\pm$ 0.056) E-2		(2.2 $\pm$ 0.3) E-2
Au-197(n,2n)Au-196m+g	3.403 $\pm$ 0.080		3.0 $\pm$ 0.3
Nb-93(n,2n)Nb-92m	(4.660 $\pm$ 0.117) E-1	(4.75 $\pm$ 0.32) E-1	(4.8 $\pm$ 0.4) E-1
I-127(n,2n)I-126	1.288 $\pm$ 0.042	1.050 $\pm$ 0.065	0.9 $\pm$ 0.1
Mn-55(n,2n)Mn-54	(2.368 $\pm$ 0.067) E-1	(2.44 $\pm$ 0.15) E-1	(2.58 $\pm$ 0.13) E-1
Co-59(n,2n)Co-58m+g	(2.036 $\pm$ 0.051) E-1		(4.0 $\pm$ 0.4) E-1
Cu-63(n,2n)Cu-62	(1.186 $\pm$ 0.073) E-1	(1.22 $\pm$ 0.12) E-1	(1.24 $\pm$ 0.11) E-1
F-19(n,2n)F-18	(8.653 $\pm$ 0.464) E-3		(7.3 $\pm$ 0.7) E-3
Zr-90(n,2n)Zr-89m+g	(1.031 $\pm$ 0.028) E-1	(2.47 $\pm$ 0.17) E-1	(0.76 $\pm$ 0.01) E-1
Ni-58(n,2n)Ni-57	(4.272 $\pm$ 0.124) E-3	(5.77 $\pm$ 0.31) E-1	(4.9 $\pm$ 1.4) E-3



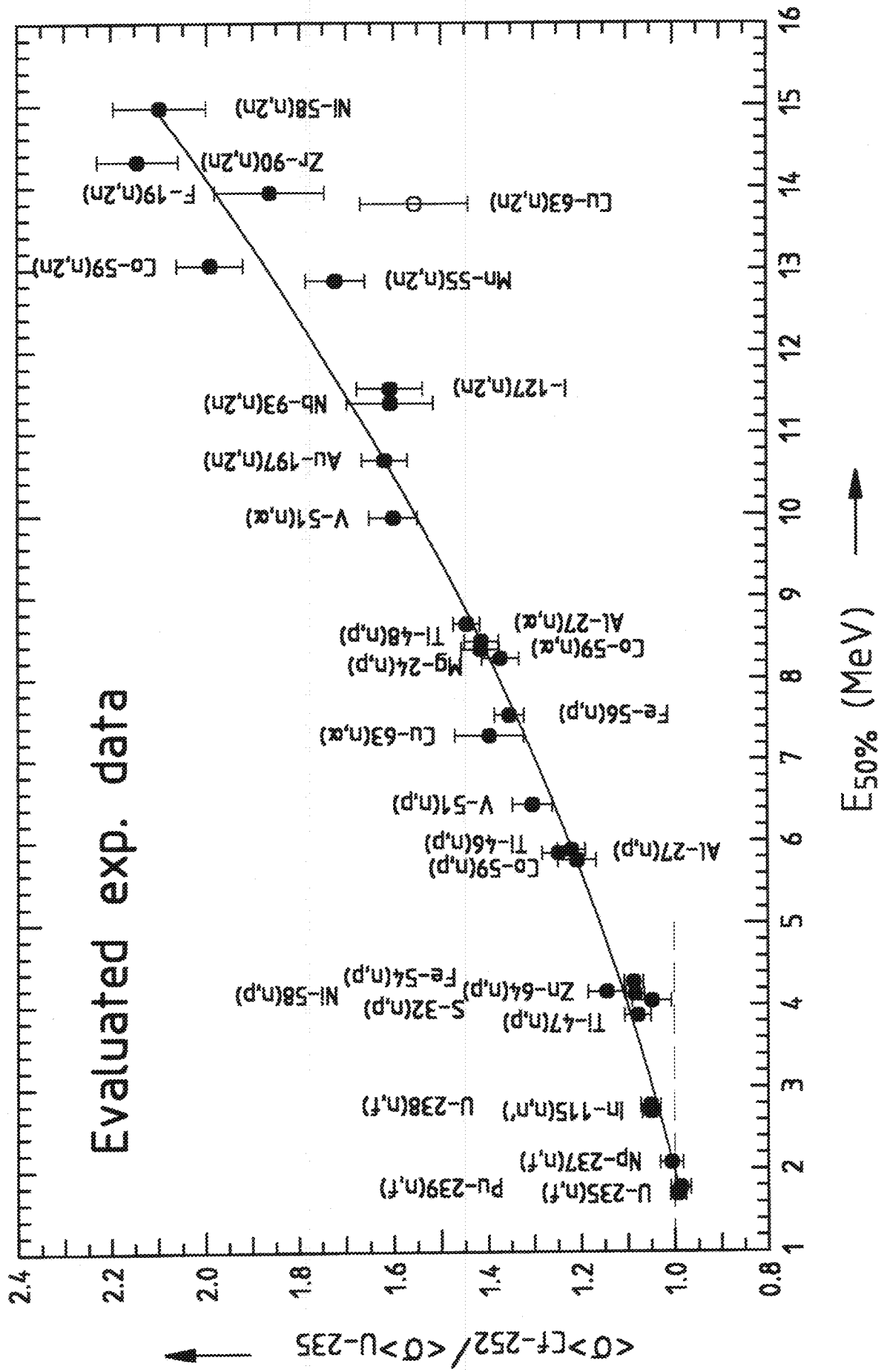


Fig. 1: Ratio of evaluated integral data in the  $^{252}\text{Cf(sf)}$  and the  $^{235}\text{U}(n_{th,e})$  neutron fields (see text).

## 2. X-Ray and $\gamma$ -Ray Emission Probabilities and Half-Life of $^{153}\text{Sm}$

U. Schötzig, E. Schönfeld, E. Günther, R. Klein, H. Schrader

X-ray and gamma-ray emission probabilities have been derived from emission rates of several sources measured with calibrated high-purity Ge and Si(Li) detectors, and from the activity which was determined by  $4\pi\beta\gamma$ -coincidence measurements and by liquid scintillation counting. The half-life has been determined by following the decay with a high-pressure  $4\pi\gamma$  ionization chamber. Results are summarized in Tables 2 and 3. Standard uncertainties are given in parentheses in terms of the last digit. For details see reference [5].

Table 2: Half-life ( $T_{1/2}$ ) of  $^{153}\text{Sm}$

$T_{1/2}$ in h	$T_{1/2}$ in d
46.274(7)	1.9281(3)

## 3. X-Ray and $\gamma$ -Ray Emission Probabilities of $^{169}\text{Yb}$

E. Schönfeld, U. Schötzig, R. Klein

X-ray and gamma-ray emission probabilities have been determined by measuring emission rates with calibrated high-purity Ge and Si(Li) detectors using sources of known activity which was determined using  $4\pi\text{EC-}\gamma$ -coincidence measurements and  $4\pi\gamma$  high efficiency counting. Results are summarized in Table 4. Standard uncertainties are given in parentheses in terms of the last digit.

Table 3: X-ray and  $\gamma$ -ray emission probabilities P (quanta per disintegration) of  $^{153}\text{Sm}$ 

Energy in keV	Radiation	P
5.15	$L_{\lambda}$	0.00216(11)
5.82	$L_{\alpha}$	0.0494(11)
6.53	$L_{\beta}$	0.0426(9)
7.57	$L_{\gamma}$	0.00615(10)
6.2	$L_{\text{total}}$	0.1003(14)
40.9	$K_{\alpha 2}$	0.1627(18)
41.5	$K_{\alpha 1}$	0.294(4)
41.3	$K_{\alpha}$	0.457(5)
47.0	$K_{\beta 1}$	0.0926(12)
48.3	$K_{\beta 2}$	0.02444(27)
47.3	$K_{\beta}$	0.1170(13)
69.67	$\gamma$	0.0465(5)
75.42	$\gamma$	0.00233(19)
83.37	$\gamma$	0.00211(11)
89.49	$\gamma$	0.00156(7)
97.43	$\gamma$	0.00755(7)
103.18	$\gamma$	0.2923(18)
151.62	$\gamma$	0.000115(6)
172.85	$\gamma$	0.000716(7)
412.05	$\gamma$	0.0000189(13)
424.4	$\gamma$	0.0000182(12)
436.9	$\gamma$	0.0000167(9)
463.6	$\gamma$	0.0001268(18)
485.0	$\gamma$	0.0000036(9)

Energy in keV	Radiation	P
509.15	$\gamma$	0.0000183(19)
521.3	$\gamma$	0.0000676(11)
531.40	$\gamma$	0.000537(6)
533.2	$\gamma$	0.0002930(27)
539.1	$\gamma$	0.0002058(25)
542.7	$\gamma$	0.0000218(17)
545.75	$\gamma$	0.000012(5)
554.94	$\gamma$	0.0000473(10)
578.75	$\gamma$	0.0000341(10)
584.55	$\gamma$	0.0000103(8)
587.60	$\gamma$	0.0000047(8)
590.96	$\gamma$	0.0000123(8)
596.7	$\gamma$	0.000104(3)
598.3	$\gamma$	0.0000206(10)
603.60	$\gamma$	0.0000436(9)
609.5	$\gamma$	0.000118(4)
615.8	$\gamma$	0.0000068(7)
617.9	$\gamma$	0.0000089(7)
634.8	$\gamma$	0.0000045(10)
636.5	$\gamma$	0.0000174(8)
657.55	$\gamma$	0.0000041(7)
686.0	$\gamma$	0.0000021(6)
713.9	$\gamma$	0.0000027(11)

Table 4: Measured relative ( $P_{rel}$ ) and absolute ( $P$ ) emission probabilities of  $^{169}\text{Yb}$ , evaluated absolute emission probabilities  $P$  (quanta per disintegration) and absolute transition probabilities  $P_{\gamma+ce}$  (including conversion electrons).  $P_{\gamma+ce}$  values are based on the evaluated relative emission probabilities, the normalization factor 0.3591 and evaluated conversion coefficients.

E in keV	Radiation	$P_{rel}$ measured	$P_{rel}$ evaluated <sup>*)</sup>	$P$ measured	$P$ evaluated	$P_{\gamma+ce}$ evaluated
6.34	Tm- $L_{\lambda}$	3.7(14)		0.013(5)		
6.8-7.6	Tm- $L_{\alpha 1,2}$	66(5)		0.237(18)		
8.1	Tm- $L_{\beta 1,3,4}$	50(4)		0.178(14)		
8.4	$\gamma$ +Tm- $L_{\beta 2}$	13.8(16)		0.050(6)		
9.4	Tm- $L_{\gamma 1}$	7.4(13)		0.027(5)		
9.8	Tm- $L_{\gamma 2,3}$	2.7(10)		0.0095(30)		
49.77	Tm- $K_{\alpha 2}$	149.1(26)		0.535(10)		
50.74	Tm- $K_{\alpha 1}$	263(5)		0.947(18)		
57.44	Tm- $K_{\beta 1}$	86(4)		0.310(15)		
59.07	Tm- $K_{\beta 2}$	22.8(11)		0.082(4)		
8.410	$\gamma$	-	0.966(45)		0.00347(16)	0.9503(10)
20.744	$\gamma$	0.539(29)	0.535(28)		0.00192(10)	0.112(7)
63.120	$\gamma$	122.7(14)	122.9(9)		0.441(4)	0.931(20)
93.614	$\gamma$	7.12(10)	7.14(6)		0.02564(23)	0.125(4)
109.779	$\gamma$	48.0(5)	48.42(24)		0.1739(11)	0.600(8)
117.377	$\gamma$	-	0.116(6)		0.000417(22)	0.00085(7)
118.189	$\gamma$	5.18(6)	5.202(27)		0.01868(12)	0.0497(10)
130.523	$\gamma$	31.57(25)	31.59(13)		0.1134(6)	0.244(5)
156.735	$\gamma$	0.029(7)	0.0275(7)		0.0000988(26)	0.000109(3)
177.213	$\gamma$	61.9(5)	62.07(26)		0.2229(12)	0.3544(28)
197.957	$\gamma$	100	100		0.3591(13)	0.520(6)
240.333	$\gamma$	0.282(15)	0.312(10)		0.00112(4)	0.00117(4)
261.077	$\gamma$	4.64(4)	4.691(19)		0.01684(10)	0.01732(10)
294.590	$\gamma$	-	0.0027(7)		0.0000097(25)	0.0000112(29)
307.736	$\gamma$	27.96(18)	27.94(10)		0.1003(5)	0.1070(6)
333.948	$\gamma$	0.0051(10)	0.00493(15)		0.0000177(6)	0.0000180(6)
336.621	$\gamma$	0.025(3)	0.0248(4)		0.0000890(14)	0.0000904(15)
370.856	$\gamma$	0.0019(6)	0.00267(10)		0.0000096(4)	0.0000125(5)

<sup>\*)</sup> Based on PTB values from 1983 and 1998 and values of six other authors determined in 1976 - 1998; for details see reference [6].

## References

- [1] D.G. Madland, Los Alamos National Laboratory, USA, priv. communication (1999)
- [2] A. Fabry, W.N. McElroy, L.S. Kellogg, E.P. Lippincott, J.A. Grundl, D.M. Gilliam, G.E. Hansen, Proc. IAEA Consultants' Meeting, Vienna, 15-19 November 1976, IAEA TECDOC-208, IAEA, Vienna (1978), p. 233
- [3] A. Calamand, in Handbook on Nuclear Activation Cross Sections, IAEA Technical Reports Series No. 156, IAEA, Vienna (1974), p. 273
- [4] W. Mannhart, Proc. of Specialists' Meeting on Evaluation and Processing of Covariance Data, Oak Ridge National Laboratory, 7-9 October 1992, Report NEA/NSC/DOC(93)3, OECD, Paris (1993), p. 157
- [5] U. Schötzig, E. Schönfeld, E. Günther, R. Klein and H. Schrader, Appl. Radiat. Isot., 1999, to be published
- [6] E. Schönfeld, U. Schötzig, R. Klein, Appl. Radiat. Isot. **50** (1999) 753



## **APPENDIX**

### **Addresses of Contributing Laboratories**

Institut für Kernphysik III  
Director: Prof. Dr. G. Schatz  
Reporter: Dr. F. Käppler  
Forschungszentrum Karlsruhe  
Postfach 36 40  
**76021 Karlsruhe**

Institut für Neutronenphysik  
und Reaktortechnik  
Director: Prof. Dr. G. Kessler  
Reporter: Dr. U. Fischer  
Forschungszentrum Karlsruhe  
Postfach 36 40  
**76021 Karlsruhe**

Institut für Nuklearchemie  
Director: Prof. Dr. H.H. Coenen  
Reporter: Prof. Dr. S.M. Qaim  
Forschungszentrum Jülich  
Postfach 1913  
**52425 Jülich**

Institut für Kern- und Teilchenphysik  
Director: Prof. Dr. B. Spaan  
Reporter: Prof. Dr. K. Seidel  
Technische Universität Dresden  
Mommensenstr. 13  
**01062 Dresden**

Zentrum für Strahlenschutz und Radioökologie  
Head and reporter: Prof. Dr. R. Michel  
Universität Hannover  
Am Kleinen Felde 30  
**30167 Hannover**

Abteilung Nuklearchemie  
Head: Prof. Dr. H.H. Coenen  
Reporter: Dr. U. Herpers  
Universität zu Köln  
Otto-Fischer-Straße 12 - 14  
**50674 Köln**



Institut für Kernchemie  
Head and reporter: Prof. Dr. H.O. Denschlag  
Universität Mainz  
Fritz-Strassmann-Weg 2  
**55128 Mainz**

FRM-Reaktorstation  
Reporter: Dr. W. Waschkowski  
Technische Universität München  
**85747 Garching/München**

Physikalisch-Technische Bundesanstalt  
Abteilung Ionisierende Strahlung  
Director: Prof. Dr. G. Dietze  
Reporter: Dr. W. Mannhart  
Bundesallee 100  
**38116 Braunschweig**

